Title: Matrix metalloproteinase-10 deficiency delays atherosclerosis progression and plaque calcification

Running title: MMP10, atherosclerosis & calcification

Ana Purroy,[1,2] Carmen Roncal,[1,2,3] Josune Orbe,[1,2,3] Olivier Meilhac,[4] Miriam Belzunce,[1,2] Guillermo Zalba,[2,5] Ricardo Villa-Bellosta,[6,7] Vicente Andrés, [3,6] William C. Parks,[8] José A. Páramo,[2,3,9] José A. Rodríguez[1,2,3]

[1]Laboratory of Atherothrombosis. Program of Cardiovascular Diseases. CIMA, University of Navarra. Pamplona, Spain.

[2]IdiSNA, Navarra Institute for Health Research, Pamplona, Spain.

[3]CIBERCV, Instituto de Salud Carlos III, Madrid, Spain.

[4]INSERM UMR698; AP-HP, Department of Neurology, Bichat Stroke Center; University Paris Diderot, Sorbonne Paris Cité, Paris F-75018, France.

[5]Department of Biochemistry and Genetics, University of Navarra, Pamplona, Spain.

[6]Centro Nacional de Investigaciones Cardiovasculares (CNIC) Carlos III, Madrid, Spain.

[7]Current address: Fundación Instituto de Investigación Sanitaria Fundación Jiménez Díaz (FIIS-FJD), Madrid, Spain.

[8]Women's Guild Lung Institute, Cedars-Sinai Medical Center, Los Angeles, CA, USA.

[9]Hematology Service, Clínica Universidad de Navarra, Pamplona, Spain.

Word count: 4940

Subject codes: Atherosclerosis pathophysiology [134], Mechanism of atherosclerosis/growth factors [96]

Corresponding author:

José A. Rodríguez

Laboratory of Atherothrombosis

Program of Cardiovascular Diseases. CIMA, University of Navarra

Av. Pio XII, 55. 31008 Pamplona (Spain)

Tel: (+34)948194700 / Fax: (+34)948194716

e-mail: josean@unav.es

Abstract *(250 words)*

Background and aims. Matrix metalloproteinases (MMPs) have been implicated in atherosclerosis and vascular calcification. Among them, we reported that MMP10 is present in human atheroma, associated with atherosclerosis. However, it remains unclear whether MMP10 is involved in atherogenesis and vascular calcification.

Methods. MMP10 was measured in serum from patients with subclinical atherosclerosis and analyzed in carotid endarterectomies by immunostaining. Apoe-deficient mice (*Apoe*$^{-/-}$) were crossed to MMP10-deficient (*Mmp10*$^{-/-}$) mice and followed up to 20 months. Plaque area and composition were assessed by histology and immunohistochemistry. Inflammatory markers were measured in atherosclerotic plaques by RT-qPCR, and leukocyte subpopulations were analyzed by flow cytometry. In vitro calcification assays were performed in aortic vascular smooth muscle cells (VSMC).

Results. MMP10 serum levels were associated with coronary calcification in subjects with subclinical atherosclerosis. Immunostaining revealed MMP10 expression in human atheromas, spatially associated with calcification areas, and complicated plaques released higher amounts of MMP10 than non-diseased segments. Interestingly, vascular MMP10 expression was confined to the atherosclerotic lesion in *Apoe*$^{-/-}$ mice, and *Apoe*$^{-/-}$*Mmp10*$^{-/-}$ showed a substantial reduction in atherosclerotic lesion size, macrophage content and plaque calcification. Reduced local and systemic inflammatory markers could be demonstrated in *Apoe*$^{-/-}$*Mmp10*$^{-/-}$ by gene expression and flow cytometry analysis. Calcium phosphate deposition and vascular calcification markers were downregulated in VSMC from *Apoe*$^{-/-}$ *Mmp10*$^{-/-}$ mice.

Conclusions. Delayed plaque progression and altered cellular composition in the absence of MMP10 suggests that MMP10 plays a role in atherosclerosis, favoring inflammation, development and complication of the plaque.

Keywords: atherosclerosis, metalloproteinases, macrophage, inflammation, calcification

Graphical Abstract

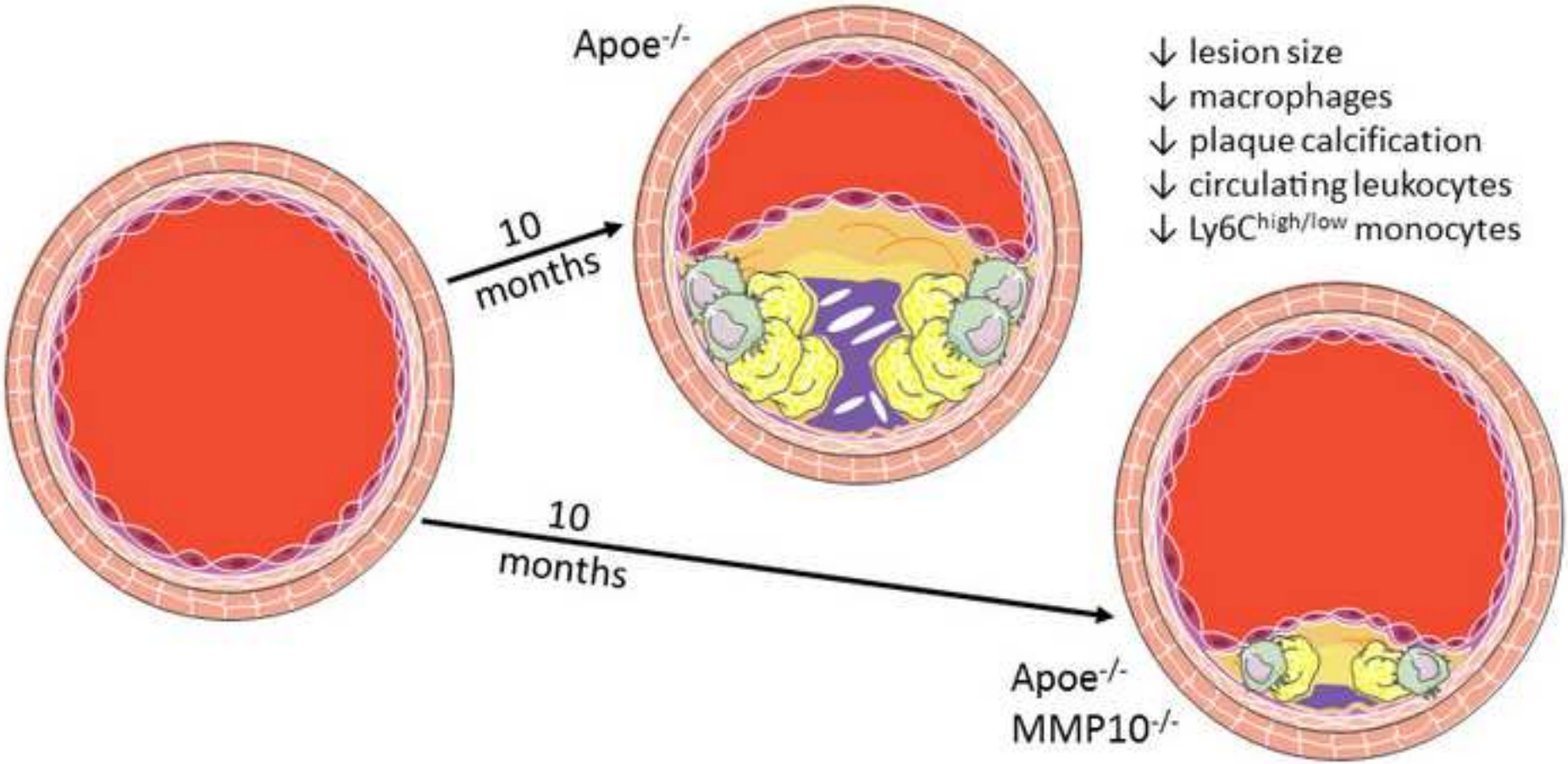

INTRODUCTION

An imbalance between proteases and their inhibitors has been hypothesized to be involved in the growth, destabilization, and eventual rupture of atherosclerotic plaques.[1] Matrix metalloproteinases (MMPs) are a group of more than 20 zinc-containing endopeptidases that are either secreted or expressed at the cell surface. MMPs can act on a wide range of extracellular proteins, including several components of the extracellular matrix (ECM).[2] There is substantial evidence indicating that MMPs play a relevant role in various physiological and pathological processes such as organ development, tissue remodelling and inflammation, particularly in atherosclerosis and its ischemic clinical manifestations such as myocardial infarction and stroke.[2] Several MMPs are locally expressed within human atherosclerotic lesions in vulnerable rupture-prone sites[3] and have also been associated with vascular calcification,[4] involving phenotypic changes of vascular smooth muscle cells (VSMC) and expression of bone-related proteins.[5,6] Macrophage infiltration and proinflammatory cytokines are essential in early stages of plaque development leading to calcification.[7]

MMP10 (stromelysin-2) has been proposed to participate in physiological processes like bone growth[8] and wound healing,[9] while its overexpression has been reported in various carcinomas and tumours,[10] and it has been suggested to be involved in vascular pathology.[11] MMP10 expressed by macrophages in response to acute infection has been shown to play a beneficial role by moderating their proinflammatory response.[12] Our group has shown that MMP10 is induced in response to injury or inflammatory stimuli,[13–15] it is present in atherosclerotic lesions at rupture-prone sites and that increased serum proMMP10 is associated with clinical and subclinical atherosclerosis.[13,16,17] However, little is known on its pathophysiological role in atherothrombosis, particularly in the development of calcified lesions.

We explored MMP10 expression in human and murine atherosclerosis [apolipoprotein E deficient (*Apoe*$^{-/-}$) mouse], and studied the effect of functional MMP10 deficiency on atherogenesis. We found that MMP10 was associated with vascular calcification in human atherosclerotic plaques and in patients with cardiovascular (CV) risk. *Apoe*$^{-/-}$*Mmp10*$^{-/-}$ mice displayed reduced atherosclerosis, decreased macrophage content and calcification. Moreover, MMP10 inactivation was associated with lower expression of pro-calcifying genes in murine

aortic VSMC. Taken together our results support a relevant role for MMP10 in modulating progression of atherosclerosis and plaque calcification.

MATERIALS AND METHODS

A detailed description is presented in the online Data Supplement.

Patients

A computed tomography (CT) scan for coronary artery calcium scoring was performed in 136 apparently healthy subjects (90% men, mean age 59±8 years), free from overt vascular disease, recruited at the time of attending the outpatient clinic for vascular risk assessment at Clínica Universidad de Navarra (Pamplona, Spain).

Human carotid endarterectomy samples (n=52), obtained from patients undergoing surgery at the Centre Cardiologique du Nord (Saint-Denis, France), were collected and dissected as described previously,[18,19] separating the culprit area of each plaque (CP) from its adjacent non-culprit plaque (NCP). MMP-10 release from atherosclerotic plaques was measured by ELISA (DuoSet, R&D Systems) in conditioned media from human endarterectomy samples incubated for 24 hours in RPMI medium. MMP-10, smooth muscle α-actin (SMA) and CD68 were analyzed by immunohistochemistry in atherosclerotic plaques from patients undergoing carotid endarterectomy (n=10). Calcium deposition was assessed by Alizarin red staining. Study protocols conform to the ethical guidelines of the 1975 Declaration of Helsinki, were approved by the Institutions' ethics committees and written informed consent was obtained from each patient included in the study.

Experimental animals

Animal experimentation was performed with wild type, *Apoe*$^{-/-}$ and *Apoe*$^{-/-}$*Mmp10*$^{-/-}$ mice (all in C57Bl/6 background). *Mmp10*$^{-/-}$ mice (B6.129P2-Mmp10^{tm1Jkmg}) were crossbred with *Apoe*$^{-/-}$ mice (B6.129P2-Apoe^{tm1Unc}/J; Charles River Laboratories, L'Arbresle Cedex, France) to obtain *Apoe*$^{-/-}$*Mmp10*$^{-/-}$ mice. Animals were maintained on standard chow diet throughout the experiment until sacrifice. Blood cell populations were analyzed by flow cytometry. All experiments were conducted according to the European Community guidelines for ethical animal care and use of laboratory animals (Directive 86/609), and were approved by the University of Navarra Animal Research Review Committee.

Analysis of Plaque Area and Composition

Aortic *en face* preparations of *Apoe*$^{-/-}$ and *Apoe*$^{-/-}$*Mmp10*$^{-/-}$ mice were used to quantify the surface area occupied by atherosclerosis. Total plaque area in the brachiocephalic artery and in the aortic root was measured on van Gieson-stained tissue sections, and calcification was

assessed by Alizarin red staining. Sirius red staining was used to quantify collagen under polarized light. VSMC and macrophage content in the aortic root and brachiocephalic artery were analyzed by immunohistochemistry.

In vitro studies

Primary cultures of aortic VSMC were established from 8-12 week-old *Apoe*$^{-/-}$ and *Apoe*$^{-/-}$ *Mmp10*$^{-/-}$ mice and in vitro calcification assays were performed. The expression of vascular calcification-related genes [alkaline phosphatase (ALPL), bone morphogenetic protein-2 (BMP2), Fetuin-A, matrix GLA protein (MGP), Osterix (Sp7) and Runx2 was assessed by reverse transcription and real time-quantitative PCR.

Statistical Analysis

Continuous variables were expressed as mean±standard deviation or median (interquartile range), unless otherwise stated. Data normality was assessed through Shapiro-Wilk's test. Serum MMP10 concentration was transformed logarithmically and its relationship with coronary calcium was analyzed by ANCOVA. Association between two variables was assessed by Pearson's correlation test (normal distribution) or Spearman's rank correlation test (non-parametric distribution). Differences between two groups were analyzed by Student's t-test when following a normal distribution or Mann-Whitney U test in case of non-parametric distribution. When comparing more than two groups, one factor ANOVA with post hoc test was used, in the case of parametric distribution, or Kruskal Wallis test followed by Mann-Whitney test with Bonferroni correction, in the case of non-parametric. The Pearson's χ^2 - test was used to compare frequency distributions of categorical variables. SPSS version 15.0 was used for the analysis, and statistical significance was established as $p<0.05$.

RESULTS

MMP10 is associated with subclinical and clinical atherosclerosis

Previous findings from our group demonstrated an association of MMP10 with CV risk factors and subclinical atherosclerosis.[13,16] Thus we analyzed the relationship between circulating MMP10 and coronary calcification, a surrogate marker of CV disease, in 136 asymptomatic subjects free from overt CV disease who underwent CT scan (baseline characteristics shown in Supplemental Table 1). Individuals with undetectable coronary calcium exhibited the lowest serum proMMP10 concentration, which increased in those with moderate and severe vascular calcification ($p<0.0001$; Figure 1A). Moreover, differences were maintained after adjusting for age, sex and smoking (ANCOVA $p<0.01$). These variables were chosen because they had been previously reported to be associated with MMP10[13,20] (univariate analysis shown in Supplemental Figure 1).

Because we had shown that MMP10 is expressed in human atheromas,[13] we further investigated the amount of total MMP10 released by human carotid endarterectomy plaques (n=52), which were separated into stenosing-culprit (CP) and adjacent non-stenosing segments (NCP) and incubated in serum-free culture medium.[18] Segments containing culprit plaques released higher amounts of MMP10 than non-complicated areas (307.3± 30.7 *vs* 224.5± 26.7 pg/ml, $p<0.01$, Figure 1B). Interestingly, among them, the highest MMP10 levels were released by CP segments of calcified haemorrhagic plaques as compared to adjacent NCP (n=9; 429.1± 67.7 vs. 151.3± 53.3 pg/ml; $p<0.01$, Figure 1C).

To analyze the tissue distribution of MMP10 in human atherosclerotic plaques, we performed immunohistochemical staining for MMP10 on sections of carotid endarterectomy samples (Figure 1D-G). MMP10 staining was limited to CD68 positive areas, although not all CD68-labeled zones were MMP10 positive. MMP10+ CD68+ tissue was spatially associated with vascular calcification, as shown by alizarin red staining in the vicinity. No MMP10 mmunostaining was observed in cells expressing α-smooth muscle actin.

Vascular MMP10 expression in murine atherosclerosis

To determine if MMP10 was associated with murine atherosclerosis, we assessed vascular MMP10 expression in wild type (*WT*) and *Apoe*$^{-/-}$ mice at different ages, receiving regular chow or hyperlipidemic diet. MMP10 mRNA was undetectable in aortas from wild-type mice at any age, irrespective of the diet, and in 4 month-old *Apoe*$^{-/-}$, when no signs of atherosclerosis were visible in this vascular bed (data not shown). However, aortic MMP10

mRNA expression was readilly detected in *Apoe*$^{-/-}$ mice at 8 months of age, marginally increased at 16 months (Figure 2A), and it was was further augmented by feeding a hyperlipidemic diet for 2 or 4 months.

Reduced atherosclerosis in MMP10 deficient mice

We assessed the role of MMP10 on murine atherosclerosis by comparing lesion size in *Apoe*$^{-/-}$ and *Apoe*$^{-/-}$*Mmp10*$^{-/-}$ mice at different vascular beds. Animals were euthanized at 6, 10 or 20 months of age, to provide a wider range of lesion stages. Compared with *Apoe*$^{-/-}$ mice, atherosclerosis burden in the aorta *en face* was significantly decreased in *Apoe*$^{-/-}$*Mmp10*$^{-/-}$ mice at 10 ($p<0.05$) and 20 months ($p<0.01$, Figure 2B), while no atherosclerotic lesions were observed in the aorta at 6 months in either genotype. After quantifying lesion area in the aortic root, *Apoe*$^{-/-}$*Mmp10*$^{-/-}$ mice exhibited a significant reduction in atheroma size at 10 months compared to *Apoe*$^{-/-}$ mice ($p<0.05$, Figure 2C). Lesion area was also significantly reduced in the brachiocephalic artery of *Apoe*$^{-/-}$*Mmp10*$^{-/-}$ mice, starting at 6 months of age ($p<0.05$) and this difference was more pronounced at 10 months, when it almost reached a 3-fold reduction ($p<0.01$, Figure 2D). No difference in total plasma cholesterol was seen between *Apoe*$^{-/-}$ or *Apoe*$^{-/-}$*Mmp10*$^{-/-}$ mice (Supplemental Table 2).

Features of atherosclerotic plaque from Apoe$^{-/-}$*Mmp10*$^{-/-}$ *mice*

Occurrence of vascular calcification, which is associated with advanced atherosclerosis, was significantly reduced in brachiocephalic lesions from *Apoe*$^{-/-}$*Mmp10*$^{-/-}$ mice (33% *vs* 86%, $p<0.05$, Figure 3A-B). Areas of calcification were much larger in *Apoe*$^{-/-}$ mice, taking up most of the lesion area, with chondrocyte-like cells situated adjacent to or within these areas of calcium deposition presenting condensed pyknotic nuclei. However, these differences disappeared at 20 months, when 100% of brachiocephalic lesions were calcified in both strains. Moreover, aortic roots were analyzed and no differences were found between *Apoe*$^{-/-}$ and *Apoe*$^{-/-}$*Mmp10*$^{-/-}$ mice in terms of calcified area as such [266.812 (204.361) *vs* 181.420 (113.469) μm^2] or relative to lesion size [29.3 (16.9) vs 22.4 (14.1)%]. The frequency of breaks in the internal elastic lamina of *Apoe*$^{-/-}$ lesions was significantly higher than in *Apoe*$^{-/-}$ *Mmp10*$^{-/-}$ (85% vs 22%; $p<0.05$) and ruptures were associated with areas of intimal calcification (Figure 2D).

Plaque composition was assessed in 10 month-old mice, when differences in plaque size were more patent. At brachiocephalic lesions, no significant differences in VSMC [0.30 (0.15)% *vs* 0.07 (0.09)%] or collagen [26.87 (27.74)% *vs* 20.82 (23.12)%] content were observed. In the

aortic root, however, atherosclerotic lesions from *Apoe*$^{-/-}$*Mmp10*$^{-/-}$ mice exhibited higher VSMC content (1.18±0.27% *vs.* 0.51±0.05%, $p<0.05$) than *Apoe*$^{-/-}$ mice (Figure 3C), with similar amount of collagen (27.23±4.86% *vs* 26.35±6.34%, $p<0.05$). Vascular calcification was not observed in the aortic root of these mice.

Reduced macrophages in Apoe$^{-/-}$*Mmp10*$^{-/-}$ *mice*

In the brachiocephalic artery, atherosclerotic plaques of *Apoe*$^{-/-}$*Mmp10*$^{-/-}$ mice exhibited a decrease in macrophage content (expressed as percentage of total lesion area) as compared to *Apoe*$^{-/-}$ mice (0.47± 0.17% *vs* 3.44± 0.64%, $p<0.01$, Figure 3D). A lower macrophage number was also observed in the aortic roots from *Apoe*$^{-/-}$*Mmp10*$^{-/-}$ mice (5.21±0.66% *vs* 12.91±3.07%, $p<0.05$, Supplemental Figure 2). Reduced macrophage infiltration found in the absence of MMP10 led us to analyze the expression of macrophage differentiation markers in the atherosclerotic plaque. For this purpose, plaques from aortic root and brachiocephalic artery were pooled and homogenized and RNA was extracted (Supplemental Figures 3 and 4). As was expected, proinflammatory markers were increased in 10-month-old *Apoe*$^{-/-}$ mice. In contrast, we found in *Apoe*$^{-/-}$*Mmp10*$^{-/-}$ samples reduced expression of mRNAs for the M1 differentiation markers IL12a ($p<0.01$), inducible NO synthase (NOS2; $p<0.05$) and TNFα ($p<0.01$; Supplemental Figure 3 A-C), while no significant changes were observed for IFNγ (Supplemental Figure 3 D). Similarly, the expression of M2 markers arginase 1 (Arg1; $p<0.01$) and IL10 ($p<0.05$) was also reduced (Supplemental Figure 3 E-F), although no changes were found in mannose receptor C-type 1 (CD206/Mrc1; Supplemental Figure 3G)

Altered MMP expression in the plaque

We analyzed the mRNA expression of MMP2 and MMP9 in the atherosclerotic plaque, looking for a potential compensation among MMPs, since they had been shown to play different roles in the *Apoe*$^{-/-}$ model of atherosclerosis.[21] While no changes were found in MMP2 (Supplemental Figure 4 A), a significant decrease in MMP9 expression was observed in 10-month-old *Apoe*$^{-/-}$*Mmp10*$^{-/-}$ mice (Supplemental Figure 4 C). Gene expression of MMP3, which shares high (82%) sequence homology with MMP10, was markedly reduced ($p<0.01$) in the absence of MMP10, both at 6 and 10 months (Supplemental Figure 4 B). TIMP1, an MMP inhibitor, followed a similar gene expression profile with reduced expression at 6 and 10 months (Supplemental Figure 4 D).

Reduced circulating CD11b+ cells in the absence of MMP10

Observed differences in the plaque's inflammatory profile led us to assess the effect of MMP10 on systemic inflammation, analyzing blood cell populations by flow cytometry. The number of circulating CD11b+ cells was reduced ($p<0.05$) in 10-month-old *Apoe*$^{-/-}$*Mmp10*$^{-/-}$ mice, in parallel with the lower granulocyte ($p<0.01$) and monocyte ($p<0.05$) counts (Figure 4A-C). Interestingly, the inflammatory Ly6C^{hi} monocyte subset was reduced ($p<0.05$) in *Apoe*$^{-/-}$*Mmp10*$^{-/-}$ mice, while Ly6C^{lo} monocytes were increased ($p<0.01$; Figure 4D-F).

MMP10 induces calcification and osteogenic gene expression in VSMC

Striking reduction in calcification observed *in vivo* in the absence of functional MMP10, led us to study its role in VSMC calcification. First of all, we could detected low MMP10 expression in VSMC from Apoe$^{-/-}$ mice by qPCR (in the range of 35 to 38 Cts) and confirmed this result in human coronary artery smooth muscle cells by *in silico* analysis of transcriptional profiles in Gene Expression Omnibus (GSE37558, Supplemental Figure 5).[22] After 14 days in culture, aortic VSMC from *Apoe*$^{-/-}$ mice had higher amount of calcium phosphate deposition as compared with *Apoe*$^{-/-}$*Mmp10*$^{-/-}$ VSMC (Figure 5A), confirming the association of MMP10 with vascular calcification. Interestingly, we could observe that the expression of alkaline phosphatase (ALPL), inducer of calcification, was reduced in these cells at 24 and 48 hours after switching to calcification medium ($p<0.05$, Figure 5B).

Next we compared the expression of pro and anti-calcifying genes in VSMC from both genotypes. We found lower bone morphogenetic protein 2 (BMP2) in *Apoe*$^{-/-}$*Mmp10*$^{-/-}$ 24 and 48 hours after switching to calcification medium ($p<0.05$, Figure 5C), accompanied by a non-significant MGP increase (Figure 5D), leading to a significantly lower BMP2/MGP ratio (Figure 5E). Accordingly, we observed that the expression of osteogenic transcription factors Runx2 and Osterix (sp7) was significantly reduced in *Apoe*$^{-/-}$*Mmp10*$^{-/-}$ VSMC (Figure 5F-G). These results together indicate an altered expression of calcification-related genes towards a less-calcifying phenotype in the absence of MMP10.

DISCUSSION

We report herein that vascular MMP10 expression in mice is restricted to the atherosclerotic lesion and that its absence is associated with a substantial reduction of atherosclerosis, decreased macrophage content and plaque calcification. We also show that increased circulating MMP10 in humans is associated with coronary calcium, further supporting its relationship with atherosclerosis progression and complications.

We confirm our previous observation that MMP10 is expressed in human atherosclerotic lesions,[13] where it colocalizes with macrophages and areas of vascular calcification. This relationship is not new for MMPs since MMP3 has been shown to colocalize with calcium and fibrin deposits in advanced symptomatic carotid lesions,[23] suggesting a possible role for both stromelysins in arterial calcification. Moreover, MMP9 also induces vascular calcification and is present in calcified carotid endarterectomy samples.[24] In the present study we demonstrated *ex vivo* that MMP10 is released from human atheroma, likely contributing to increased serum MMP10 levels reported in patients with atherosclerosis.[16,17] Maximal MMP10 secretion observed in calcified haemorrhagic plaques, in agreement with the positive correlation found between MMP10 and coronary calcification, strengthens the association of MMP10 with the progression and complications of atherosclerosis.

MMPs have been proposed to play a main role in atherosclerotic plaque remodelling and rupture. Augmented expression of many MMPs has been observed in plaque tissues, being monocytes and macrophages their main producers either constitutively or in response to inflammatory mediators,[2] but little attention has been paid to MMP10. We could clearly show that MMP10 expression is associated with the atherosclerotic process, since MMP10 could not be detected in ApoE-null mice until atherosclerotic plaques are present, and in wild type animals at any age. Critically, this suggests that MMP10 does not play a role in regulating initiation of atherosclerosis, but may play an important role in modulating progression of atherosclerosis. However, since MMPs have multiple roles and a variety of matrix and non-matrix substrates, their local overexpression does not necessarily imply a causal role in atherosclerotic plaque progression. Research conducted in experimental models of atherosclerosis and genetically modified mice has shown that different members of the MMP family play divergent roles in atherosclerotic plaque development and destabilization.[25] Apoe deficient mice lacking functional MMP10 exhibited reduced

atherosclerotic lesion size at the three vascular beds studied (thoracic aorta, aortic root and brachiocephalic artery), confirming our hypothesis. Smaller lesions observed in mice suggest that the atherosclerosis process is delayed in the absence of functional MMP10. Moreover, atherosclerotic plaques from *Apoe*$^{-/-}$*Mmp10*$^{-/-}$ mice also showed decreased macrophage content and more VSMC, indicating overall lower inflammation and a more stable phenotype. The absence of differences in collagen content further supports that MMP10 functions in atherosclerosis are not limited to the mere degradation of the ECM components of the plaque. Interestingly, belonging to the same group of metalloproteinases than MMP10 and despite their high degree of homology (82%) and similar substrate specificity, mice with a combined deficiency of Apoe and MMP3 showed larger lesions throughout the thoracic aorta[26] and brachiocephalic artery.[25] *Apoe*$^{-/-}$*Mmp3*$^{-/-}$ lesions, in contrast with *Apoe*$^{-/-}$*Mmp10*$^{-/-}$, showed lower VSMC content in the brachiocephalic artery but increased collagen content and macrophage accumulation in the thoracic aorta.(23) It must be also noticed that genetic deletion of MMP-11 (stromelysin-3) had no effect on lesion size in mice.[27]

Lower incidence of vascular calcification and breaks in the internal elastic lamina, indicate that *Apoe*$^{-/-}$*Mmp10*$^{-/-}$ mice display a less inflamed and more stable plaque phenotype. Moreover, reduced expression of the M1 macrophage polarization markers IL12a, NOS2 and TNFα in the plaques of *Apoe*$^{-/-}$*Mmp10*$^{-/-}$ mice could also indicate reduced local inflammation in the absence of MMP10. However, we have also encountered lower expression of Arg1 and Il10 so that reduced macrophage content, likely consequence of diminished monocyte infiltration or local (intraplaque) macrophage proliferation, may explain the lower frequency of internal elastic lamina ruptures and differences in macrophage polarization profiles. Remarkably, our results are in agreement with recent reports demonstrating that macrophages from *Mmp10*$^{-/-}$ mice display reduced migration and invasion into fibronectin matrix.[28] Speculating that monocyte chemotactic mechanisms could be altered in the absence of MMP10, we should highlight the importance of the chemokine receptor CXCR4 and its ligand CXCL12 mediating the homing of progenitor cells in the bone marrow and regulating their mobilization and recruitment.[29] We have previously shown that MMP10 modulates CXCR4/CXCL12 signaling after acute skeletal muscle injury[30] and their reciprocal crosstalk in mouse hepatocarcinogenesis[31]: CXCL12 induced MMP10 expression in hepatocellular carcinoma (HCC) cells and the stimulation of HCC cell migration by MMP10 was reduced with a CXCR4 inhibitor.

Reduced neutrophilia and monocytosis encountered in the absence of MMP10 would suggest that systemic inflammation, characteristic of this model of murine hypercholesterolemia, is also attenuated. Moreover, *Apoe*$^{-/-}$*Mmp10*$^{-/-}$ mice show higher abundance of patrolling Ly6C^{lo} and less Ly6C^{hi} monocytes. This subset, displaying a more pro-inflammatory profile, has been shown to accumulate in the circulation of *Apoe*$^{-/-}$ mice and to be recruited preferentially into atherosclerotic plaques.[32,33] Interestingly, our results are in stark contrast with the increased macrophage infiltration and predominant M1 polarization observed in *Mmp10*$^{-/-}$ mice after bacterial infection.[12] Differences between the acute inflammatory response to infection and chronic inflammation in atherosclerosis could account for the apparent disparity in the results, but in both cases MMP10 is involved in the control of macrophage activation.

Inflammation and, particularly, macrophages have been demonstrated to participate in the calcification process,[7] so reduced macrophage content might also explain lower plaque calcification and fewer chondrocyte-like cells observed in *Apoe*$^{-/-}$*Mmp10*$^{-/-}$ mice; however, a direct involvement of MMP10 in this process cannot be excluded. Vascular calcification reflects an osteochondrogenic transformation of VSMC, which is facilitated by several factors, including cytokines and bone morphogenetic proteins, such as TNFα and BMP2, which can induce ALPL, a key factor for soft tissue biomineralization. In contrast, MGP is a negative regulator of calcification by direct binding of calcium phosphate nano-crystals, preventing their aggregation and also by inhibition of BMP-2 by direct binding.[34] Pathological calcification is the consequence of the imbalance between inducers and inhibitors, and MMPs have been proposed to be implicated in this process but the exact roles of individual MMPs are poorly understood.[35] We have found reduced calcification in the absence of functional MMP10 *in vivo* and also *in vitro*, in VSMC, suggesting that MMP10 could be involved in this process. These results are in agreement with reports demonstrating that the interaction of MMP10 with BMP2 signaling pathway enhances osteoblastic differentiation *in vitro*[36] and bone repair *in vivo*[37], and also with the impaired atherosclerotic calcification observed in MMP2 deficient mice.[38] Since BMP2 has been shown to be produced by VSMC in the plaque,[39] it could be hypothesized that MMP10 locally produced by macrophages could be enhancing pro-osteogenic effects of BMP2, thus promoting plaque calcification. Reduced calcification could result from diminished BMP2/MGP ratio, promoting a subsequent decrease in ALPL expression, accompanied by the down-regulation of Osterix and Runx2 found in *Apoe*$^{-/-}$*Mmp10*$^{-/-}$ VSMC.

In spite of the solid evidence provided associating MMP10 with atherosclerosis, we acknowledge that our research work has several limitations that should be addressed in future studies. Mainly, the experimental evidence obtained *in vivo* does not allow us to rule out that the reduced calcification observed in 10 month-old $Apoe^{-/-}Mmp10^{-/-}$ mice could be secondary to the delayed plaque development and reduced macrophage infiltration. The mechanisms responsible for the differences in monocyte/macrophage activation and the phenotypic switch in VSMC remain to be defined. Besides, the indirect effects derived from the proteolytic activation of MMP-1, -7, -8 and -9 by MMP10 should be also taken into account. Moreover, given the ability of MMP3 for releasing active TNFα from the cell surface, the involvement of MMP10 in TNFα shedding should be also properly assessed. Further studies are warranted to define more precisely the functions of MMP10 in atherosclerosis.

In summary, the present study demonstrates that MMP10 plays a relevant role in atherogenesis by favoring plaque inflammation, development and complication, providing further evidence of MMPs involvement in atherosclerosis.

CONFLICT OF INTEREST

The authors declared they do not have anything to disclose regarding conflict of interest with respect to this manuscript.

SOURCES OF FUNDING

Funded through the "UTE project CIMA" (University of Navarra), Ministerio de Educación y Ciencia (SAF2009-12039, SAF2016-79151-R), Ministerio de Sanidad y Consumo (PI14/01152 and PI15/01807), Sociedad Española de Cardiología, Sociedad Española de Arteriosclerosis, Red de Investigación Cardiovascular RIC (RD12/0042/0009), the Fondation pour la Recherche Médicale and the Fondation de France.

AUTHOR CONTRIBUTIONS

AP and CR designed and performed experiments, analyzed data, and wrote the manuscript. MB, RVB, OM and JO performed experiments and analyzed data. GZ, VA, WCP and JAP analyzed data and revised the manuscript. JAR designed experiments, interpreted data, wrote the manuscript and supervised this study.

ACKNOWLEDGEMENTS

We want to thank Dr. Oscar Beloqui (Clínica Universidad de Navarra, Pamplona, Spain) for providing data and serum samples from healthy subjects, Lara Montori for her excellent technical assistance, Dr. Jean B. Michel (Inserm, UMR 698, Paris 7-Denis Diderot University, CHU X. Bichat, Paris, France) and vascular surgeons from the Centre Cardiologique du Nord (St Denis, France) for providing carotid samples. We also thank personnel at Imaging Core Facility (CIMA) for their support.

FIGURE LEGENDS

Figure 1. MMP10 is associated with clinical and subclinical atherosclerosis. (**A**) Increased serum MMP10 in asymptomatic subjects with higher coronary calcification score. Median ± IQR. *** P< 0.001 vs T1; ††† P< 0.001 vs T2. (**B**) Human atherosclerotic plaques (n=52) express and secrete MMP10. Stenosing-culprit segments (CP) of carotid plaques release more MMP10 than the adjacent non-culprit ones (NCP). (**C**) MMP10 levels were maximal in the subgroup of calcified haemorrhagic carotid plaques (n=9). * P< 0.05; ** P< 0.01. Median and interquartilic range. Panels **D** shows MMP10 immunostaining of a human carotid endarterectomy, partially colocalizing with CD68 (**E**) and alizarin red (**F**), but there is no overlapping with smooth muscle α-actin staining (**G**).

Figure 2. Vascular MMP10 is expressed during atherosclerotic plaque development and its functional inactivation reduces plaque growth. (**A**) Vascular MMP10 mRNA expression in wild type (*WT*) and *Apoe*$^{-/-}$ mouse aorta, with or without hyperlipidemic diet (mean ± SD; n=5 per genotype and time point). * P<0.05 *vs* 8 month-old *Apoe*$^{-/-}$ mice. (**B**) Representative images of *en face* preparations of aortas from 10-month-old *Apoe*$^{-/-}$ and *Apoe*$^{-/-}$*Mmp10*$^{-/-}$ mice and chart with the proportion of atherosclerotic aortic surface in the two groups of mice. (**C**, **D**) Representative images of Van Gieson-stained aortic roots (**C**) and brachiocephalic arteries (**D**), charts show plaque area in both vascular localizations. A higher number of internal elastic lamina breaks can be noticed in *Apoe*$^{-/-}$ mice (magnification of panel **D**). * P< 0.05; ** P< 0.01 vs *Apoe*$^{-/-}$ mice. Median and interquartilic range.

Figure 3. Plaque composition is altered in *Apoe*$^{-/-}$*Mmp10*$^{-/-}$ mice, showing features of increased stability. Representative images of brachiocephalic arteries (**A**, **B**, **D**) and aortic root (**C**) from 10 month-old *Apoe*$^{-/-}$ and *Apoe*$^{-/-}$*Mmp10*$^{-/-}$ mice. Panels **A** and **B** show calcification in sections stained with hematoxylin-eosin and alizarin red respectively. Arrows point to chondrocyte-like cells next and within large calcified areas. The graph on the right side shows the frequency of calcified plaques with its confidence interval. Panel **C** shows VSMC content in the neointima (α-smooth muscle actin immunostaining and quantification as percent of total lesion area). Panel **D** shows macrophage content (F4/80 immunostaining and quantification as percent of total lesion area) in the two groups of mice. * P< 0.05; ** P< 0.01 vs *Apoe*$^{-/-}$. Median and interquartilic range.

Figure 4. Reduced systemic inflammation in 10-month-old *Apoe*$^{-/-}$ mice in the absence of MMP10. **A**) Leukocyte population was gated based on CD11b staining and quantified in both genotypes. **B**) CD11b+ cells were further divided and counted as **C**) granulocytes (Ly6G+CD115-) and **D**) monocytes (CD115+, Ly6G-). (**E-G**) Monocyte subsets were classified based on Ly6C staining as Ly6C^{low}, Ly6C^{int} and Ly6C^{high}. n=9 per group, Median and interquartilic range. *P<0.05, **P<0.01.

Figure 5: Reduced calcification and altered expression of calcification-related genes in VSMC from *Apoe*$^{-/-}$*Mmp10*$^{-/-}$ mice. **(A)** Reduced calcification in aortic VSMC from *Apoe*$^{-/-}$ *Mmp10*$^{-/-}$ in comparison with VSMC from *Apoe*$^{-/-}$ mice, as shown by Alizarin red staining. Stronger red/orange colour corresponds to calcium cell deposition. VSMC from *Apoe*$^{-/-}$ *Mmp10*$^{-/-}$ exhibit reduced ALPL (**B**) and BMP2 mRNA expression (**C**), a non-significant MGP increase (**D**), leading to lower BMP2/MGP ratio(**E**). Expression of osteogenic transcription factors Osterix **(F)** and Runx2 **(G)** are also reduced. *****, P<0.05 and **, P<0.01 *vs* *Apoe*$^{-/-}$. Median and interquartilic range from 5 independent experiments.

REFERENCES

[1] P. Libby, P.M. Ridker, G.K. Hansson, L.T.N. on Atherothrombosis, Inflammation in atherosclerosis: from pathophysiology to practice, J. Am. Coll. Cardiol. 54 (2009) 2129–2138. doi:10.1016/j.jacc.2009.09.009; 10.1016/j.jacc.2009.09.009.

[2] A.C. Newby, Dual role of matrix metalloproteinases (matrixins) in intimal thickening and atherosclerotic plaque rupture, Physiol. Rev. 85 (2005) 1–31. doi:10.1152/physrev.00048.2003.

[3] M.M. Sadeghi, D.K. Glover, G.M. Lanza, Z.A. Fayad, L.L. Johnson, Imaging atherosclerosis and vulnerable plaque, J. Nucl. Med. 51 Suppl 1 (2010) 51S–65S. doi:10.2967/jnumed.109.068163; 10.2967/jnumed.109.068163.

[4] C.L. Irwin, R.J. Guzman, Matrix metalloproteinases in medial arterial calcification: potential mechanisms and actions., Vascular. 17 Suppl 1 (2009) S40-4. http://www.ncbi.nlm.nih.gov/pubmed/19426608 (accessed June 15, 2018).

[5] D. Proudfoot, J.D. Davies, J.N. Skepper, P.L. Weissberg, C.M. Shanahan, Acetylated low-density lipoprotein stimulates human vascular smooth muscle cell calcification by promoting osteoblastic differentiation and inhibiting phagocytosis, Circulation. 106 (2002) 3044–3050.

[6] R.C. Shroff, C.M. Shanahan, The vascular biology of calcification, Semin. Dial. 20 (2007) 103–109. doi:10.1111/j.1525-139X.2007.00255.x.

[7] C.M. Shanahan, Inflammation ushers in calcification: a cycle of damage and protection?, Circulation. 116 (2007) 2782–2785. doi:10.1161/CIRCULATIONAHA.107.749655.

[8] N. Ortega, D.J. Behonick, Z. Werb, Matrix remodeling during endochondral ossification, Trends Cell Biol. 14 (2004) 86–93. doi:10.1016/j.tcb.2003.12.003.

[9] S.E. Gill, W.C. Parks, Metalloproteinases and their inhibitors: regulators of wound healing, Int. J. Biochem. Cell Biol. 40 (2008) 1334–1347. doi:10.1016/j.biocel.2007.10.024.

[10] J.H. Gill, I.G. Kirwan, J.M. Seargent, S.W. Martin, S. Tijani, V.A. Anikin, A.J. Mearns, M.C. Bibby, A. Anthoney, P.M. Loadman, MMP-10 is overexpressed, proteolytically active, and a potential target for therapeutic intervention in human lung carcinomas, Neoplasia. 6 (2004) 777–785. doi:10.1593/neo.04283.

[11] J.A. Rodriguez, J. Orbe, S. Martinez de Lizarrondo, O. Calvayrac, C. Rodriguez, J. Martinez-Gonzalez, J.A. Paramo, Metalloproteinases and atherothrombosis: MMP-10 mediates vascular remodeling promoted by inflammatory stimuli, Front Biosci. 13 (2008) 2916–2921.

[12] R.S. McMahan, T.P. Birkland, K.S. Smigiel, T.C. Vandivort, M.G. Rohani, A.M. Manicone, J.K. McGuire, S.A. Gharib, W.C. Parks, Stromelysin-2 (MMP10) Moderates Inflammation by Controlling Macrophage Activation, J. Immunol. (Baltimore, Md. 1950). 197 (2016) 899–909. doi:10.4049/jimmunol.1600502 [doi].

[13] I. Montero, J. Orbe, N. Varo, O. Beloqui, J.I. Monreal, J.A. Rodriguez, J. Diez, P. Libby, J.A. Paramo, C-reactive protein induces matrix metalloproteinase-1 and -10 in human endothelial cells: implications for clinical and subclinical atherosclerosis, J Am Coll Cardiol. 47 (2006) 1369–1378.

[14] J. Orbe, J.A. Rodriguez, O. Calvayrac, R. Rodriguez-Calvo, C. Rodriguez, C. Roncal,

S. Martinez de Lizarrondo, J. Barrenetxe, J.C. Reverter, J. Martinez-Gonzalez, J.A. Paramo, Matrix metalloproteinase-10 is upregulated by thrombin in endothelial cells and increased in patients with enhanced thrombin generation, Arter. Thromb Vasc Biol. 29 (2009) 2109–2116.

[15] M. Bobadilla, N. Sainz, J.A. Rodriguez, G. Abizanda, J. Orbe, A. de Martino, J.M. Garcia Verdugo, J.A. Paramo, F. Prosper, A. Perez-Ruiz, MMP-10 is required for efficient muscle regeneration in mouse models of injury and muscular dystrophy, Stem Cells. 32 (2014) 447–461. doi:10.1002/stem.1553; 10.1002/stem.1553.

[16] J. Orbe, I. Montero, J.A. Rodriguez, O. Beloqui, C. Roncal, J.A. Paramo, Independent association of matrix metalloproteinase-10, cardiovascular risk factors and subclinical atherosclerosis, J Thromb Haemost. 5 (2007) 91–7.

[17] B. Coll, J.A. Rodriguez, L. Craver, J. Orbe, M. Martinez-Alonso, A. Ortiz, J. Diez, O. Beloqui, M. Borras, J.M. Valdivielso, E. Fernandez, J.A. Paramo, Serum levels of matrix metalloproteinase-10 are associated with the severity of atherosclerosis in patients with chronic kidney disease, Kidney Int. 78 (2010) 1275–1280.

[18] A. Leclercq, X. Houard, S. Loyau, M. Philippe, U. Sebbag, O. Meilhac, J.B. Michel, Topology of protease activities reflects atherothrombotic plaque complexity, Atherosclerosis. 191 (2007) 1–10. doi:10.1016/j.atherosclerosis.2006.04.011.

[19] J.L. Martin-Ventura, M.C. Duran, L.M. Blanco-Colio, O. Meilhac, A. Leclercq, J.-B. Michel, O.N. Jensen, S. Hernandez-Merida, J. Tuñón, F. Vivanco, J. Egido, Identification by a differential proteomic approach of heat shock protein 27 as a potential marker of atherosclerosis., Circulation. 110 (2004) 2216–9. doi:10.1161/01.CIR.0000136814.87170.B1.

[20] J.A. Paramo, O. Beloqui, J.A. Rodriguez, J. Diez, J. Orbe, Association between matrix metalloproteinase-10 concentration and smoking in individuals without cardiovascular disease, Rev Esp Cardiol. 61 (2008) 1267–1273.

[21] A.C. Newby, S.J. George, Y. Ismail, J.L. Johnson, G.B. Sala-Newby, A.C. Thomas, Vulnerable atherosclerotic plaque metalloproteinases and foam cell phenotypes, Thromb. Haemost. 101 (2009) 1006–1011. doi:09061006 [pii].

[22] R.D.A.M. Alves, M. Eijken, J. van de Peppel, J.P.T.M. van Leeuwen, Calcifying vascular smooth muscle cells and osteoblasts: independent cell types exhibiting extracellular matrix and biomineralization-related mimicries., BMC Genomics. 15 (2014) 965. doi:10.1186/1471-2164-15-965.

[23] A. Bini, K.G. Mann, B.J. Kudryk, F.J. Schoen, Noncollagenous bone matrix proteins, calcification, and thrombosis in carotid artery atherosclerosis, Arterioscler. Thromb. Vasc. Biol. 19 (1999) 1852–1861.

[24] C. Bouvet, S. Moreau, J. Blanchette, D. de Blois, P. Moreau, Sequential activation of matrix metalloproteinase 9 and transforming growth factor beta in arterial elastocalcinosis, Arterioscler. Thromb. Vasc. Biol. 28 (2008) 856–862. doi:10.1161/ATVBAHA.107.153056; 10.1161/ATVBAHA.107.153056.

[25] J.L. Johnson, S.J. George, A.C. Newby, C.L. Jackson, Divergent effects of matrix metalloproteinases 3, 7, 9, and 12 on atherosclerotic plaque stability in mouse brachiocephalic arteries, Proc. Natl. Acad. Sci. U. S. A. 102 (2005) 15575–15580. doi:10.1073/pnas.0506201102.

[26] J. Silence, F. Lupu, D. Collen, H.R. Lijnen, Persistence of atherosclerotic plaque but

reduced aneurysm formation in mice with stromelysin-1 (MMP-3) gene inactivation, Arterioscler. Thromb. Vasc. Biol. 21 (2001) 1440–1445.

[27] H.R. Lijnen, B. Van Hoef, I. Vanlinthout, M. Verstreken, M.C. Rio, D. Collen, Accelerated neointima formation after vascular injury in mice with stromelysin-3 (MMP-11) gene inactivation, Arterioscler. Thromb. Vasc. Biol. 19 (1999) 2863–2870.

[28] M.Y. Murray, T.P. Birkland, J.D. Howe, A.D. Rowan, M. Fidock, W.C. Parks, J. Gavrilovic, Macrophage Migration and Invasion Is Regulated by MMP10 Expression, PLoS One. 8 (2013) e63555. doi:10.1371/journal.pone.0063555; 10.1371/journal.pone.0063555.

[29] Y. Döring, L. Pawig, C. Weber, H. Noels, The CXCL12/CXCR4 chemokine ligand/receptor axis in cardiovascular disease, Front. Physiol. 5 (2014) 212. doi:10.3389/fphys.2014.00212.

[30] M. Bobadilla, N. Sainz, G. Abizanda, J. Orbe, J.A. Rodriguez, J.A. Paramo, F. Prosper, A. Perez-Ruiz, The CXCR4/SDF1 Axis Improves Muscle Regeneration Through MMP-10 Activity, Stem Cells Dev. 23 (2014) 1417–1427. doi:10.1089/scd.2013.0491 [doi].

[31] O. García-Irigoyen, M.U. Latasa, S. Carotti, I. Uriarte, M. Elizalde, R. Urtasun, U. Vespasiani-Gentilucci, S. Morini, P. Benito, J.M. Ladero, J.A. Rodriguez, J. Prieto, J. Orbe, J.A. Páramo, M.G. Fernández-Barrena, C. Berasain, M.A. Avila, Matrix Metalloproteinase 10 Contributes To Hepatocarcinogenesis in a Novel Crosstalk With the Stromal Derived Factor 1/C-X-C Chemokine Receptor 4 Axis, Hepatology. 62 (2015) 166–178. doi:10.1002/hep.27798.

[32] I. Hilgendorf, F.K. Swirski, C.S. Robbins, Monocyte fate in atherosclerosis, Arterioscler. Thromb. Vasc. Biol. 35 (2015) 272–279. doi:10.1161/ATVBAHA.114.303565 [doi].

[33] F.K. Swirski, P. Libby, E. Aikawa, P. Alcaide, F.W. Luscinskas, R. Weissleder, M.J. Pittet, Ly-6Chi monocytes dominate hypercholesterolemia-associated monocytosis and give rise to macrophages in atheromata, J. Clin. Invest. 117 (2007) 195–205. doi:10.1172/JCI29950 [doi].

[34] A.P. Sage, Y. Tintut, L.L. Demer, Regulatory mechanisms in vascular calcification, Nat. Rev. 7 (2010) 528–536. doi:10.1038/nrcardio.2010.115; 10.1038/nrcardio.2010.115.

[35] X. Qin, M.A. Corriere, L.M. Matrisian, R.J. Guzman, Matrix metalloproteinase inhibition attenuates aortic calcification, Arterioscler. Thromb. Vasc. Biol. 26 (2006) 1510–1516. doi:10.1161/01.ATV.0000225807.76419.a7.

[36] L. Mao, M. Yano, N. Kawao, Y. Tamura, K. Okada, H. Kaji, Role of matrix metalloproteinase-10 in the BMP-2 inducing osteoblastic differentiation., Endocr. J. 60 (2013) 1309–19. http://www.ncbi.nlm.nih.gov/pubmed/24077220 (accessed June 14, 2018).

[37] R. Reyes, J.A. Rodríguez, J. Orbe, M.R. Arnau, C. Évora, A. Delgado, Combined sustained release of BMP2 and MMP10 accelerates bone formation and mineralization of calvaria critical size defect in mice, Drug Deliv. 25 (2018) 750–756. doi:10.1080/10717544.2018.1446473.

[38] T. Sasaki, K. Nakamura, K. Sasada, S. Okada, X.W. Cheng, T. Suzuki, T. Murohara, K. Sato, M. Kuzuya, Matrix metalloproteinase-2 deficiency impairs aortic

atherosclerotic calcification in ApoE-deficient mice, Atherosclerosis. 227 (2013) 43–50. doi:10.1016/j.atherosclerosis.2012.12.008; 10.1016/j.atherosclerosis.2012.12.008.

[39] A.Y. Simões Sato, G.L. Bub, A.H. Campos, BMP-2 and -4 produced by vascular smooth muscle cells from atherosclerotic lesions induce monocyte chemotaxis through direct BMPRII activation, Atherosclerosis. 235 (2014) 45–55. doi:10.1016/j.atherosclerosis.2014.03.030.

Ref.: Ms. No. ATH-D-18-00382R1

Matrix metalloproteinase-10 deficiency delays atherosclerosis progression and plaque calcification

Reviewers' comments:

Reviewer #2: After the first revision the manuscript ATH-D-18-00382R1 has improved significantly, and eliminated most questionable presentations and discussions of the results provided, at least in the response to the reviewers.

However, questions of reviewers should not be considered as only personal, rather as an example of questions an average reader of the article would be wondering about and therefore it would be appropriate to find the information provided to the reviewers also reflected in the manuscript, so that any reader could profit from it.

In particular the response to the question, whether the observed reduced calcification at a certain time point of plaque investigation might be a result of the reduced size of the plaques, indicated that the impression of the authors is that the calcification areas are similar, and they would interpret reduced lesion size and calcification at 10m as delayed atherosclerotic lesion development.

Thus, since the authors could not provide evidence that the calcification in plaques of similar size is reduced in MMP10 deficient mice, they can not exclude that the reduced calcification is secondary the delayed plaque development, which might be secondary to a reduced amount of macrophages in the plaque, which in turn might be secondary to a reduced amount of Ly6C-high and other monocytes in the circulation.

Bord et al., found 1998, for example, SL-2(=MMP10) in most mononuclear cells within the marrow. (Bone, Vol.23; 7-12)

A participation of MMP10 in the calcification of plaques is an intriguing possibility supported by other activities of this enzyme and the currently provided results represent many indications for this idea. However, the related discussion should be kept at this level and, while a clear effect of MMP10 on plaque development and inflammation is out of question, the effect on calcification toned down in highlights, abstract and discussion accordingly.

We appreciate the reviewer's suggestions, which we believe have contributed significantly to improving the quality of the manuscript.

We recognize that we do not provide in vivo evidence to discern a direct effect of MMP10 on plaque calcification that could not be explained by delayed plaque development. Following reviewer's suggestions, the effect of MMP10 on calcification has been toned down in highlights, abstract and discussion. We have also incuded a sentence explaining this limitation of the study.

Moreover, to reflect in the manuscript the answers provided to the reviewers, the information regarding MMP10 expression in VSMC has been included in the results and supplemental data (supplental figure 5), adding a new bibliographic reference

Changes to the text are shown in red.

Figure(s)
Figure 1

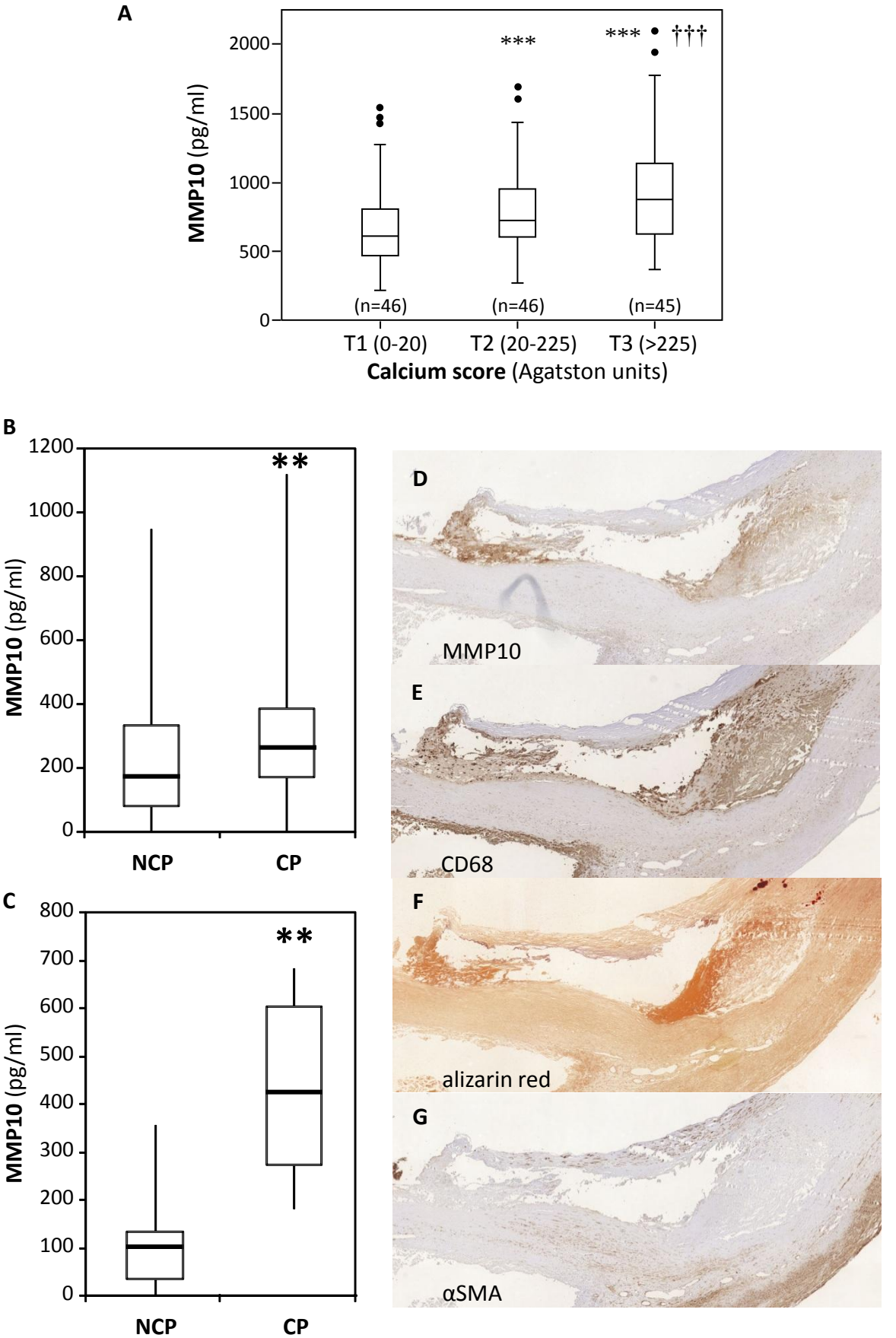

Figure 2

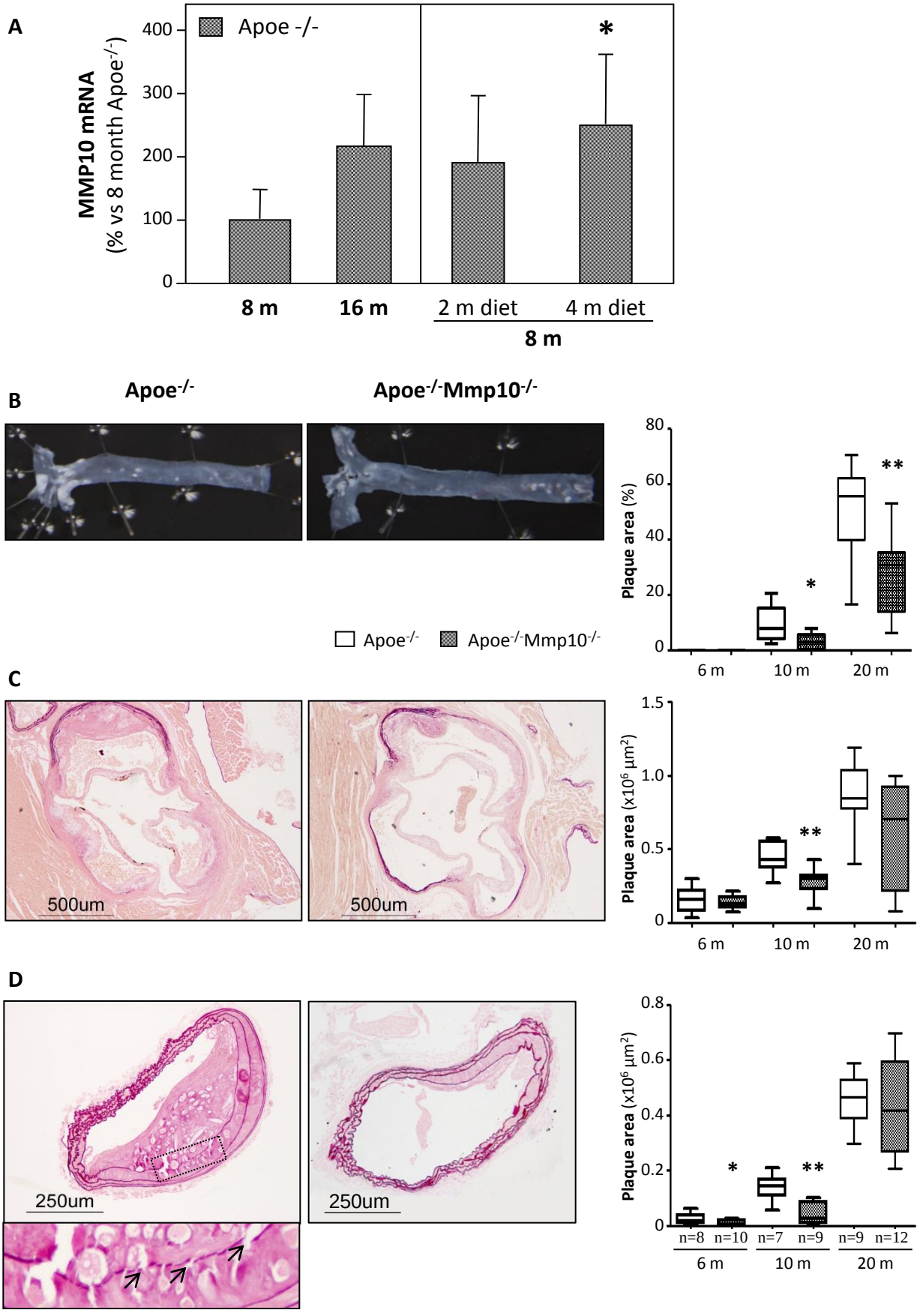
A
Apoe -/-
MMP10 mRNA
(% vs 8 month Apoe-/-)
400
300
200
100
0
*
8 m
16 m
2 m diet
4 m diet
8 m
B
Apoe-/-
Apoe-/-Mmp10-/-
Apoe-/-
Apoe-/-Mmp10-/-
Plaque area (%)
80
60
40
20
0
*
**
6 m
10 m
20 m
C
500um
500um
Plaque area (x10^6 µm^2)
1.5
1.0
0.5
0
**
6 m
10 m
20 m
D
250um
250um
Plaque area (x10^6 µm^2)
0.8
0.6
0.4
0.2
0
*
**
n=8
n=10
n=7
n=9
n=9
n=12
6 m
10 m
20 m

Figure 3

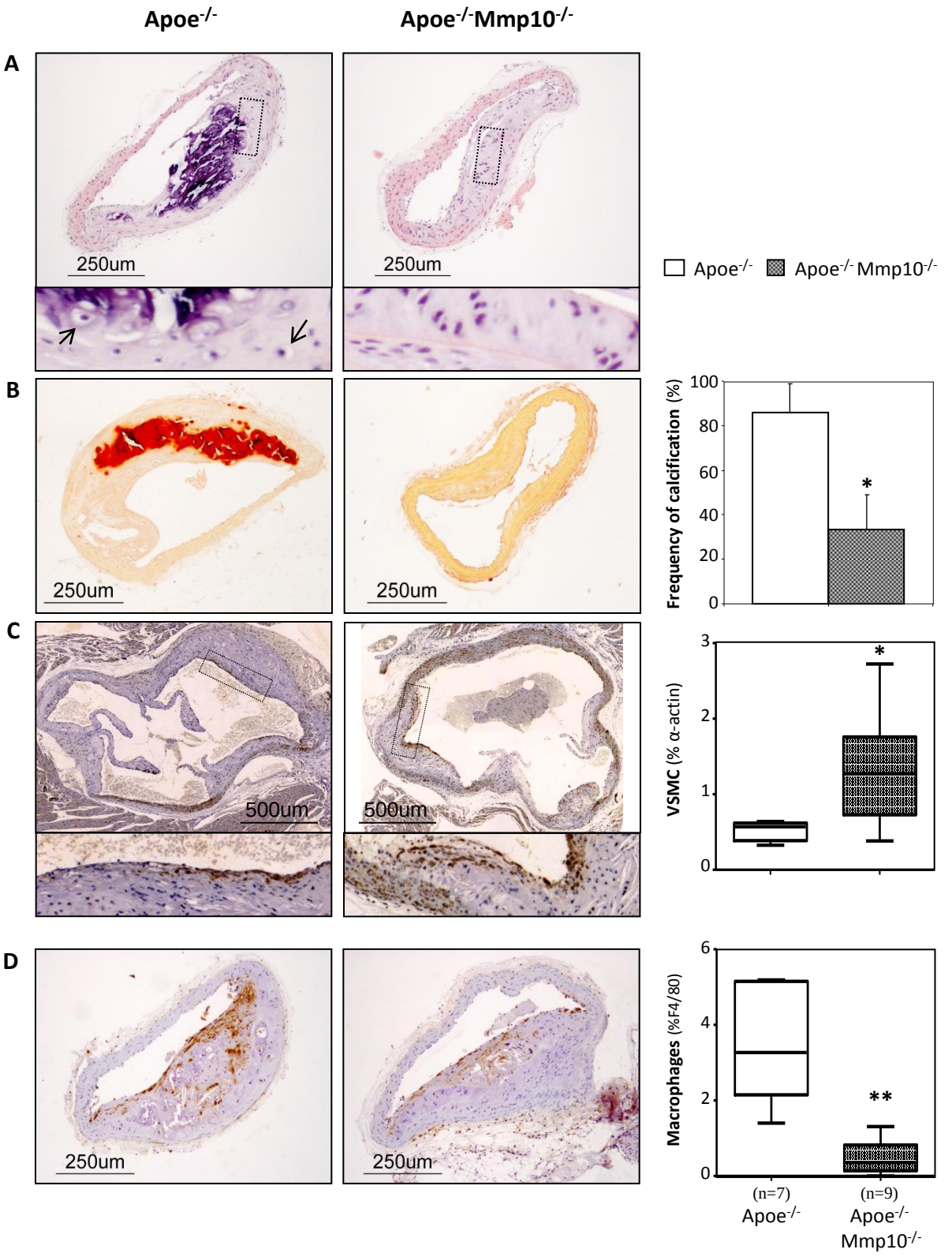
Apoe-/-
Apoe-/-Mmp10-/-
A
250um
250um
Apoe-/- Apoe-/- Mmp10-/-
B
250um
250um
Frequency of calcification (%)
100
80
60
40
20
0
*
C
500um
500um
VSMC (% α-actin)
3
2
1
0
*
D
250um
250um
Macrophages (%F4/80)
6
4
2
0
**
(n=7)
Apoe-/-
(n=9)
Apoe-/-
Mmp10-/-

Figure 4

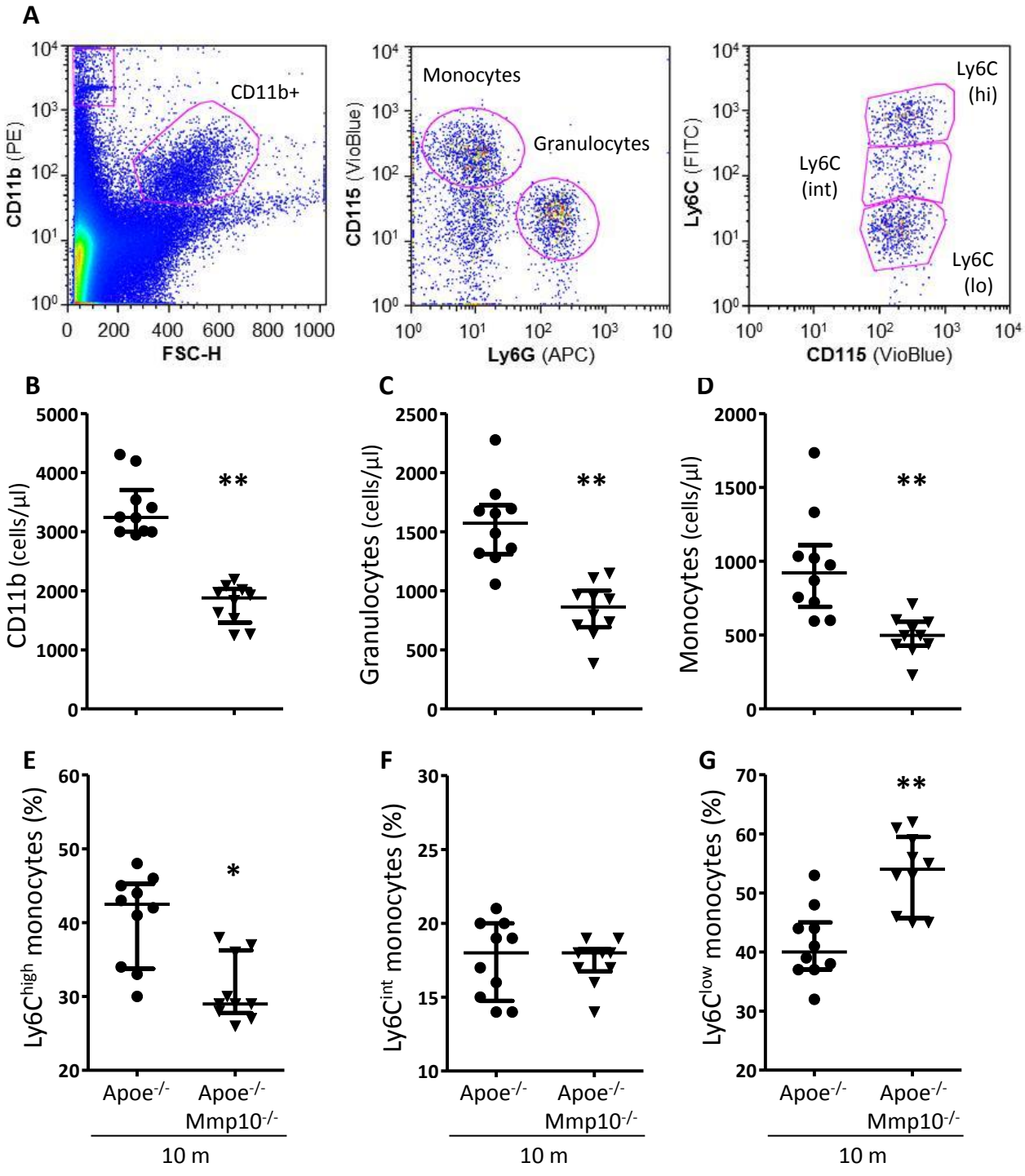
A
CD11b+
CD11b (PE)
FSC-H
Monocytes
Granulocytes
CD115 (VioBlue)
Ly6G (APC)
Ly6C (hi)
Ly6C (int)
Ly6C (lo)
Ly6C (FITC)
CD115 (VioBlue)
B
CD11b (cells/µl)
C
Granulocytes (cells/µl)
D
Monocytes (cells/µl)
E
Ly6C^high monocytes (%)
F
Ly6C^int monocytes (%)
G
Ly6C^low monocytes (%)
Apoe-/-
Apoe-/- Mmp10-/-
10 m

Figure 5

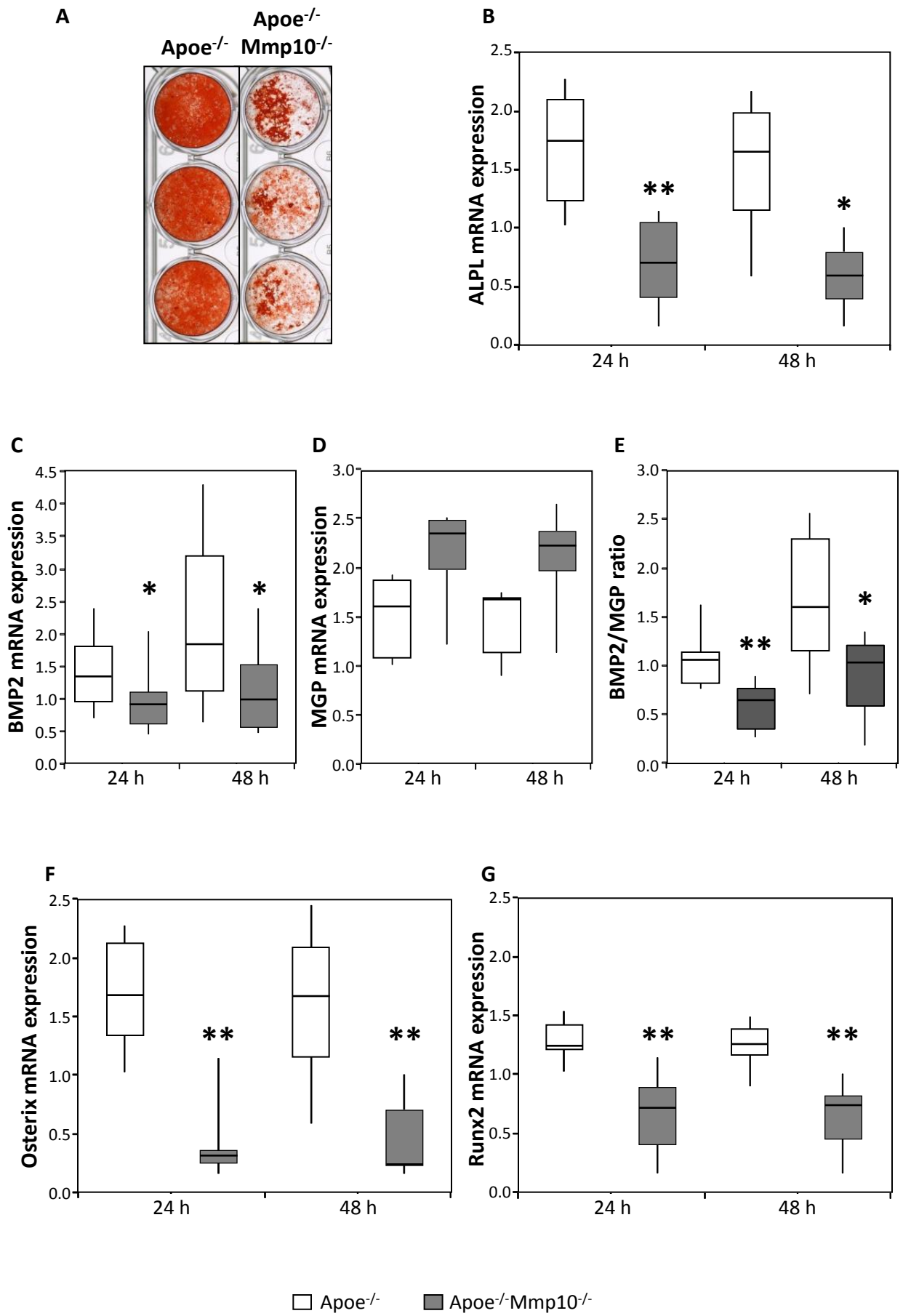
A
Apoe-/-
Apoe-/- Mmp10-/-
B
ALPL mRNA expression
24 h
48 h
C
BMP2 mRNA expression
D
MGP mRNA expression
E
BMP2/MGP ratio
F
Osterix mRNA expression
G
Runx2 mRNA expression
Apoe-/-
Apoe-/-Mmp10-/-

Supplementary Material for online publication only

Click here to download Supplementary Material for online publication only: Supplemental data file 2018-09.docx

SUPPLEMENTAL DATA FILE

MATERIAL AND METHODS

Subjects with subclinical atherosclerosis

A total of 136 apparently healthy subjects (90% men, mean age 59±8 years) were recruited at the time of attending the outpatient clinic for vascular risk assessment in the Internal Medicine Department at Clínica Universidad de Navarra (Pamplona, Spain). Subjects were free from clinically manifest atherosclerotic vascular disease on the basis of the following criteria: (i) absence of history of coronary disease, stroke or peripheral arterial disease; and (ii) normal ECG and chest X-ray results. Coronary heart disease was defined by: (i) clinical history of myocardial infarction, angina, or use of nitroglycerin; and (ii) clinical history of coronary angioplasty or coronary artery bypass surgery. Cerebrovascular disease was defined as clinical history of stroke, transient ischemic attack, or carotid endarterectomy. Patients were questioned about symptoms of intermittent claudication in a questionnaire, and in the physician's interview. Exclusion criteria were the presence of severely impaired renal function (glomerular filtration rate<30 ml/min), chronic inflammatory conditions, and administration of anti-inflammatory, antithrombotic, or hormonal therapy in the previous 2 weeks. Patients with significant acute infection, according to clinical criteria applied by the attending physician, were also excluded.

Computed tomography scan for coronary artery calcium scoring was performed using a Multislice CT scan (Volume Zoom, Siemens, Erlangen, Germany) with retrospective ECG-gating. The protocol used was collimation 4 x 2.5, with 3 mm slice thickness, table feed 3.75 mm, R.I. 1.5 mm and a kernel value of B35f. No contrast media was used. Coronary artery calcium was identified as a dense area in the coronary artery with an attenuation of 130 Hounsfield units (HU). Coronary artery calcium score was calculated using dedicated software (Heartbeat-CS, Extended Brilliance Workspace, Philips Medical System, Best, The Netherlands). Patients were divided into four groups according to Agatston score: very low (0), low (1-100), intermediate (101-400) and high (> 400).

MMP-10 secretion by human atheroma

Human carotid (n=52) endarterectomy samples were obtained from patients undergoing surgery were obtained from the Centre Cardiologique du Nord (Saint-Denis, France). These tissues are considered surgical waste in accordance with French ethical laws (L.1211.2 to L.1211.7, L.1235.2, and L.1245.2) and the INSERM Ethics Committee. Tissue samples were

collected in cold RPMI medium 1640 (Life Technologies, Paisley, UK) containing antibiotics and antimycotics (penicillin-streptomycin and amphotericin, Life Technologies) and processed within 2 hours after surgery. The investigation conforms to the principles outlined in the Declaration of Helsinki.

Carotid endarterectomy samples were dissected as previously described,[1] separating the culprit-stenosing plaque (CP) from the adjacent nonstenosing plaque (NCP). In accordance with the classification established by Stary et al,[2] histological characteristics of our samples showed that CPs represented advanced type V or VI atherothrombotic lesions. The adjacent area, considered NCP, corresponded to type III or IV lesions.

Small pieces of tissue (≈ 10 mm^3) were weighed and incubated for 24 hours in RPMI medium 1640 containing 1% L-glutamine, 1% penicillin, streptomycin, and amphotericin at 37 ºC. For standardization, the volume of medium was adjusted to sample wet weight (6 mL/g). Conditioned media from tissues were collected and then centrifuged (3000 g for 10 minutes at 20 ºC) and stored at –80 ºC until further analysis.

Immunostaining of human atherosclerotic lesions

MMP10, smooth muscle α-actin (SMA) and CD68 were analyzed by immunohistochemistry in atherosclerotic plaques from patients undergoing carotid endarterectomy (n=10). Study protocol was approved by Universidad de Navarra Institutional Ethics Committee and written informed consent was obtained from all patients. Carotid endarterectomy specimens were paraformaldehyde (4%) fixed, decalcified in Osteosoft (Merck) for 48 h and paraffin embedded. 3-μm-thick serial sections were analyzed by immunohistochemistry as previously described,[3] using rabbit polyclonal antibody anti-MMP-10 (Acris Antibodies, Germany), mouse monoclonal smooth muscle α-actin (SMA; clone 1A4, Dako, Glostrup, Denmark) and CD68 (clone KP1, Dako). Specimens were incubated with species-appropriate biotinylated secondary antibodies: EnVision rabbit or mouse horseradish peroxidase-conjugated (EnVision+/HRP, Dako). Immunocomplexes were detected with 3,3' diaminobenzidine and nuclei were counterstained with Harris´ hematoxylin. Serial sections were also analyzed by Alizarin red staining for calcium detection.

Enzyme-Linked Immunosorbent Assay

MMP-10 levels were assayed in conditioned media by human total MMP-10 ELISA kit (DuoSet, R&D Systems, Abingdon, UK) and in serum from asymptomatic subjects by human

Pro-MMP10 Immunoassay (R&D Systems). All samples were tested in duplicate according to the manufacturer's instructions. Serum samples were diluted 1:2.

Mice

Wild type C57Bl6 and apolipoprotein E-deficient ($Apoe^{-/-}$) mice (B6.129P2-$Apoe^{tm1Unc}$/J, Charles River Laboratories, L'Arbresle Cedex, France) were kept on normal chow, euthanized at 4, 8 and 16 months of age (n=5) and aortas were extracted. Some of the animals euthanized at 8 months received a hyperlipidemic diet (supplemented with 20% butter and 0.1% cholesterol) for 2 or 4 months (n=5).

Functional MMP10-deficient ($Mmp10^{-/-}$) mice (B6.129P2-$MMP10^{tm1Jkmg}$),[4] generated at the Center for Lung Biology (University of Washington, Seattle, USA) and bred in the Center for Applied Medical Research (CIMA, Pamplona, Spain) animal facilities, were crossbred with $Apoe^{-/-}$ mice to obtain $Apoe^{-/-}Mmp10^{-/-}$ mice, and their genotype was determined by polymerase chain reaction. Male $Apoe^{-/-}$ and $Apoe^{-/-}Mmp10^{-/-}$ mice were fed a normal chow, housed in a temperature-controlled room with a 12-hour light/dark cycle, with free access to water and food. Groups of 10 animals were euthanized at 6, 10 and 20 months. Blood was drawn afterwards by cardiac puncture and citrated plasma was immediately isolated by centrifugation. Plasma total cholesterol was measured with a Cobas C311 analyzer (Roche). The investigation was performed in accordance with the European Union (EU) and Spanish rules (86/609/CEE, 2003/65/CE, 2010/63/EU and RD53/2013), and was approved by the University of Navarra Ethics Committee for Animal Research.

Analysis of Plaque Area and Composition

Aortic en face preparations of $Apoe^{-/-}$ and $Apoe^{-/-}Mmp10^{-/-}$ mice were used to quantify the surface area occupied by atherosclerosis. In order to analyze plaque area and composition in the aortic root and brachiocephalic artery from $Apoe^{-/-}$ and $Apoe^{-/-}Mmp10^{-/-}$ mice, vascular samples were fixed in 4% paraformaldehyde (4 h), dehydrated and paraffin embedded. Serial cross sections (3 μm) were obtained for histological analysis. Total plaque area was measured on van Gieson-stained slides, and calcification was assessed after Alizarin red staining. Sirius red staining was used to quantify collagen under polarized light.

VSMCs and macrophage content in the aortic root and brachiocephalic artery was analyzed by immunohistochemistry with the following primary antibodies: rabbit polyclonal antibody anti-α-smooth muscle actin (Abcam, Cambridge, UK), rat monoclonal antibody against macrophages (F4/80, AbD Serotec, Oxford, UK). After primary antibody incubation,

specimens were incubated with species-appropriate biotinylated secondary antibodies: EnVision rabbit horseradish peroxidase-conjugated (Dako) and goat anti rat (AbD Serotec) followed by Tyramide Signal Amplification kit (TSA biotin system, PerkinElmer, Waltham, MA, USA) respectively. Immunocomplexes were detected with 3,3' diaminobenzidine and nuclei were counterstained with Harris´ hematoxylin. All plaque components were expressed as percentage of total plaque area. Images were analyzed with a colour image analysis program developed with MatLab (MathWorks, Natick, MA, USA).

Cell isolation and culture

Aortic VSMCs were prepared from thoracic aortas of 8- to 12-week-old Apoe$^{-/-}$ and Apoe$^{-/-}$;Mmp-10$^{-/-}$ mice as described previously.[5] Aortas were dissected free from surrounding tissue and adventitia and cut into small pieces, that were digested with 0.5 mg/ml collagenase A and grown in minimal essential medium (MEM) containing 1 mmol/L L-glutamine, 100 IU/mL penicillin, 100 µg/mL streptomycin, and 10% fetal bovine serum (FBS) at 37°C in a humidified atmosphere at 5% CO_2. Cell culture reagents were from Life Technologies.

In vitro calcification

Apoe$^{-/-}$ and Apoe$^{-/-}$;Mmp-10$^{-/-}$ VSMCs (passages 5 to 10) were grown to confluence and used after an overnight quiescence step (0.1% FBS). Calcification assays were performed on cells incubated for 14 days in MEM supplemented with 0.1% FBS and 2 mmol/L Pi, with medium change every 48 h, as described previously.[5] Cells were fixed in 4% paraformaldehyde for 10 minutes and Alizarin red stained.

RNA was extracted from VSMCs 24 or 48 h after switching to calcifying culture medium and vascular calcification-related genes were measured by real time PCR.

Real-Time PCR

RNA was extracted from cells or tissue samples using MagMAX-96 Total RNA Isolation Kit (ThermoFisher) and reverse transcription was performed with 1 µg of total RNA, random primers and Moloney murine leukaemia virus reverse transcriptase (ThermoFisher). Real-time quantitative PCR was performed on an ABI PRISM 7900 sequence detector (ThermoFisher) using TaqMan gene expression assays-on-demand (ThermoFisher) for murine MMP-10 (Mm00444630_m1), BMP2 (Mm01340178_ml), ALPL (Mm00475834_ml), MGP (Mm00485009_ml), and PrimeTime qPCR assays (IDT, Leuven, Belgium) for murine Arg1 (Mm.PT.58.8651372), Il10 (Mm.PT.58.13531087), Il12a (Mm.PT.58.13818295), interferon-γ (Mm.PT.58.41769240), Mrc-1 (Mm.PT.58.42560062), MMP2 (Mm.PT.58.9606100), MMP3

(Mm.PT.58.9719290), MMP9 (Mm.PT.58.8295969g), NOS2 (Mm.PT.58.43705194), osterix (Mm.PT.56a.10898265), Runx2 (Mm.PT.56a.11948210), TIMP1 (Mm.PT.58.30682575) and TNFα (Mm.PT.47.12575861). Murine β-actin (4352341E, ThermoFisher) was used to normalize results

Flow cytometry

Blood samples were obtained by retro-orbital venous sinus bleeding. Whole blood was stained with PE rat anti mouse CD11b (BD Bioscience), APC rat anti mouse Ly6G (BD Bioscience), FITC rat anti mouse Ly6C (BD Bioscience), CD115-PE-Vio770, mouse (Miltenyi Biotec) antibodies. After the staining, erythrocytes were cleared with FACS Lysing Solution (BD Biosciences). Finally cells were acquired on a BD FACSCalibur flow cytometer (BD Biosciences) and analyzed using FlowJo software (Tree Star Inc.). Calibrated beads (Perfect-Count Microspheres™, Cytognos) were used to calculate cell numbers.

Statistical Analysis

Continuous variables were expressed as mean±standard deviation or median (interquartile range) (IQR), unless otherwise stated. Data normality was assessed through Shapiro-Wilk's test. Serum MMP10 concentration was transformed logarithmically and its relationship with coronary calcium was analyzed by ANCOVA. Association between two variables was assessed by Pearson's correlation test (normal distribution) or Spearman's rank correlation test (non-parametric distribution). Differences between two groups were analyzed by Student's t-test when following a normal distribution or Mann-Whitney U test in case of non-parametric distribution. When comparing more than two groups, one factor ANOVA with post hoc test was used, in the case of parametric distribution, or Kruskal Wallis test followed by Mann-Whitney test with Bonferroni correction, in the case of non-parametric. The Pearson's χ^2 - test was used to compare frequency distributions of categorical variables. Boxplot graphs show median, IQR (box), the lowest datum still within 1.5 IQR of the lower quartile and the highest datum still within 1.5 IQR of the upper quartile (whiskers). SPSS version 15.0 was used for the analysis, and statistical significance was established as $p<0.05$.

Supplemental Table 1. Baseline characteristics of the patients

		Tertiles according to coronary calcium		
Coronary calcium*	77 (327)	**1st tertil** 0 (0)	**2nd tertil** 84 (105)	**3rd tertil** 878 (507)
N	137	46	46	45
Age	59±8	54±7	59±5**	65±7***†††
Weight±kg	85±14	85±17	85±12	85±14
BMI	29±4	29±4	29±4	29±4
Male n (%)	124 (90)	39 (85)	41 (89)	44 (98)
Smoker n (%)	39 (29)	16 (35)	14 (31)	9 (21)
SAP±mm Hg	133±19	130±22	131±18	138±17
DAP±mm Hg	82±9	82±8	82±9	82±8
Glucose	107±30	106±33	104±25	110±33
TC±mg/dL	216±44	225±40	229±50	194±33***†††
LDL±mg/dL	141±43	152±39	153±47	118±32***†††
HDL±mg/dL	50±15	49±12	52±19	50±14
TG* (mg/dL)	103 (69)	114 (72)	97 (82)	111 (52)
Creatinin	0.98±0.20	0.94±0.14	0.95±0.18	1.07±0.25**†
Urine albumin	1.1 (2.7)	0.8 (1.4)	1.3 (2.1)	1.1 (4.8)
Urine creatinin	149 (80)	169 (94)	144 (73)	141 (74)
MMP10* (pg/mL)	723 (425)	606 (336)	718 (347)	878 (507)
Treatments n (%)				
ACEi	16 (12)	2 (4)	5 (11)	9 (20)
ARA	29 (21)	3 (7)	9 (20)	17 (38)**
Statin	36 (27)	7 (16)	7 (16)	22 (49)***†††
Antidiabetics	16 (12)	3 (7)	4 (9)	9 (20)

Data shown as average±standard deviation or (*) median (interquartilic range).

BMI, body mass index; SAP, sistolic arterial pressure; DAP, diastolic arterial pressure; TC, total cholesterol; LDL, low density lipoprotein; HDL, high density lipoprotein; ACEi, angiotensin-converting enzyme inhibitor; ARA, angiotensin II receptor antagonists. Coronary calcium expressed in Agatston units. Comparisons vs 1st tertile are denoted as: ** p<0.01; *** p<0.001. Comparisons vs 2nd tertile are denoted as: † p<0.05; ††† p<0.001

Supplemental table 2: Total cholesterol levels in different groups of animals (expressed as mean ± SD).

Total cholesterol (mg/dL)	**6 months**	**10 months**	**20 months**
***Apoe*$^{-/-}$**	409 ± 171	495 ± 198	348 ± 102
***Apoe*$^{-/-}$*Mmp10*$^{-/-}$**	412 ± 100	469 ± 96	357 ± 192

Supplemental figure 1

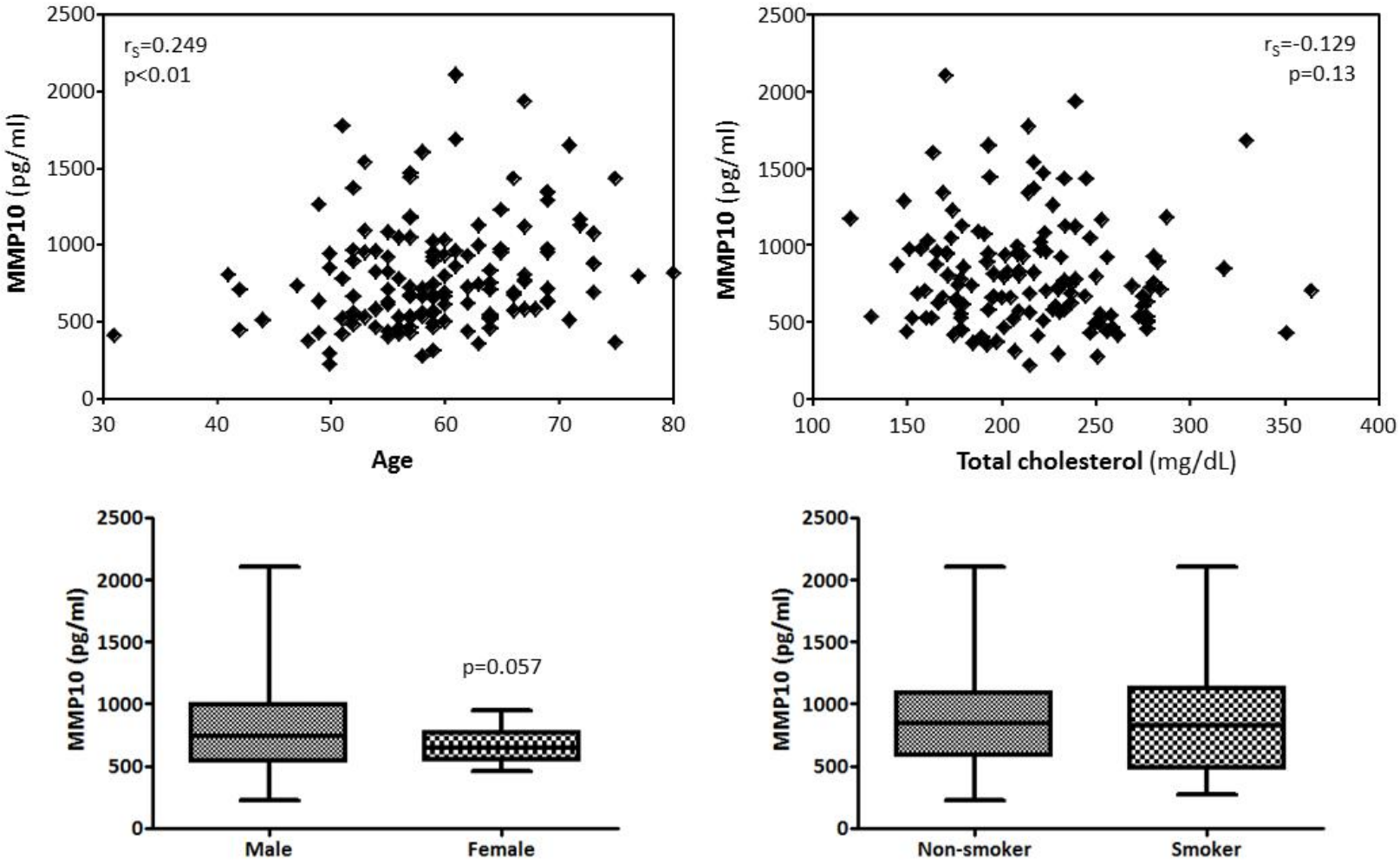

Supplemental figure 1. Association between MMP10 and other variables was initially explored by univariate analysis. Boxplots show median and interquartilic range.

Supplemental figure 2

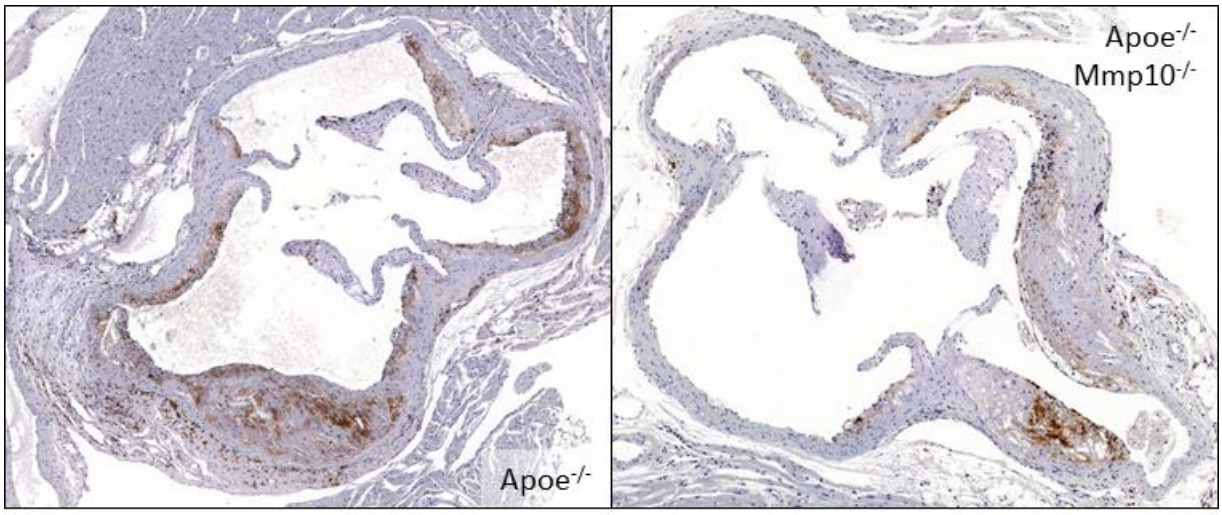

Supplemental figure 2. Representative images of F4/80 immunostaining showing lower macrophage infiltration in the aortic roots from 10 month-old $Apoe^{-/-}$;$Mmp10^{-/-}$, as compared to $Apoe^{-/-}$ mice.

Supplemental figure 3

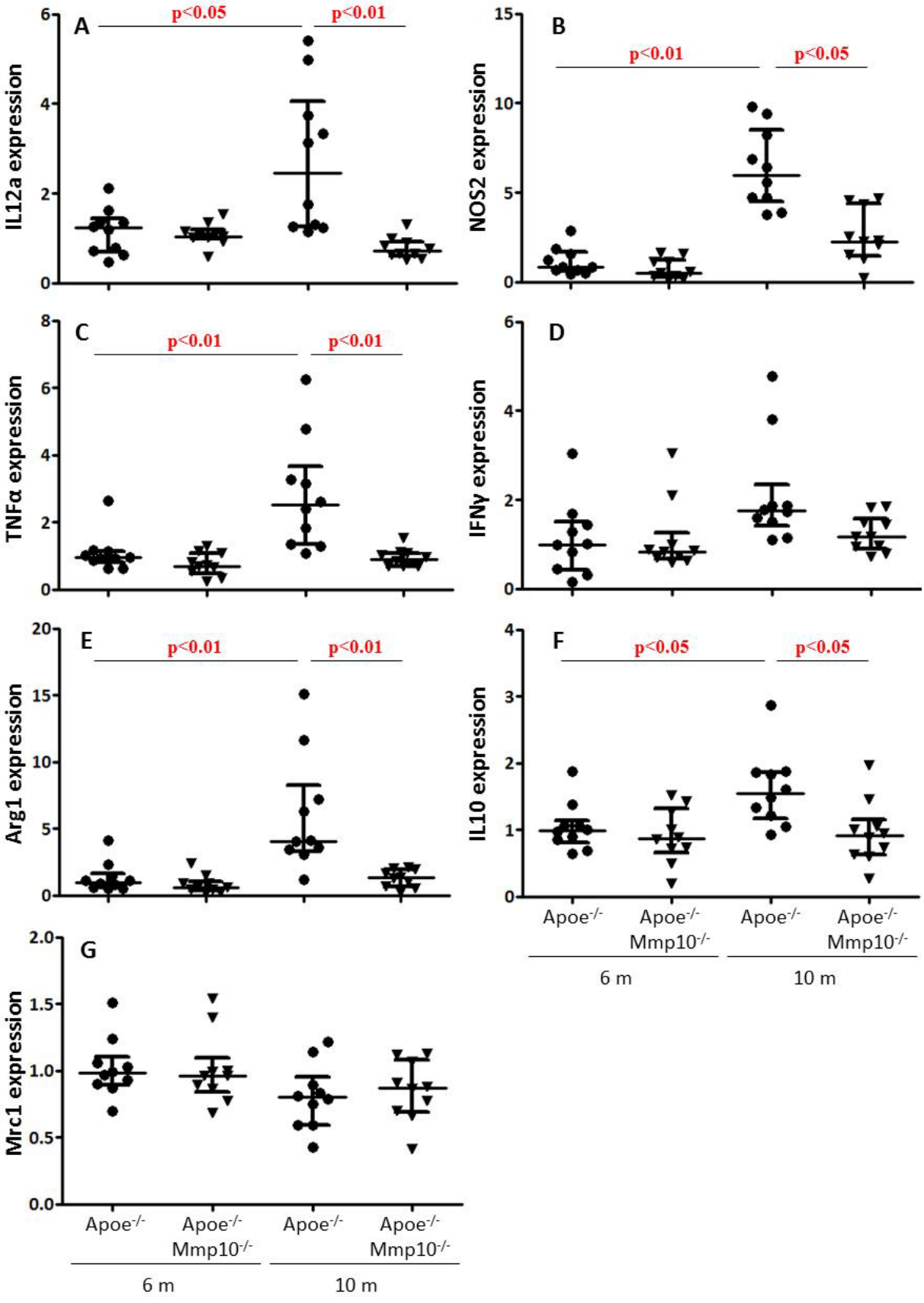

Supplemental figure 3. Altered mRNA expression of macrophage polarization markers in atherosclerotic plaques from 10 month-old *Apoe*$^{-/-}$*Mmp10*$^{-/-}$ mice. (**A-D**) proinflammatory (M1) markers IL12a, NOS2 TNFα and IFNγ. (**E-G**) M2 markers Arg1, IL10 and Mrc1. Median and interquartilic range; n=10.

Supplemental figure 4

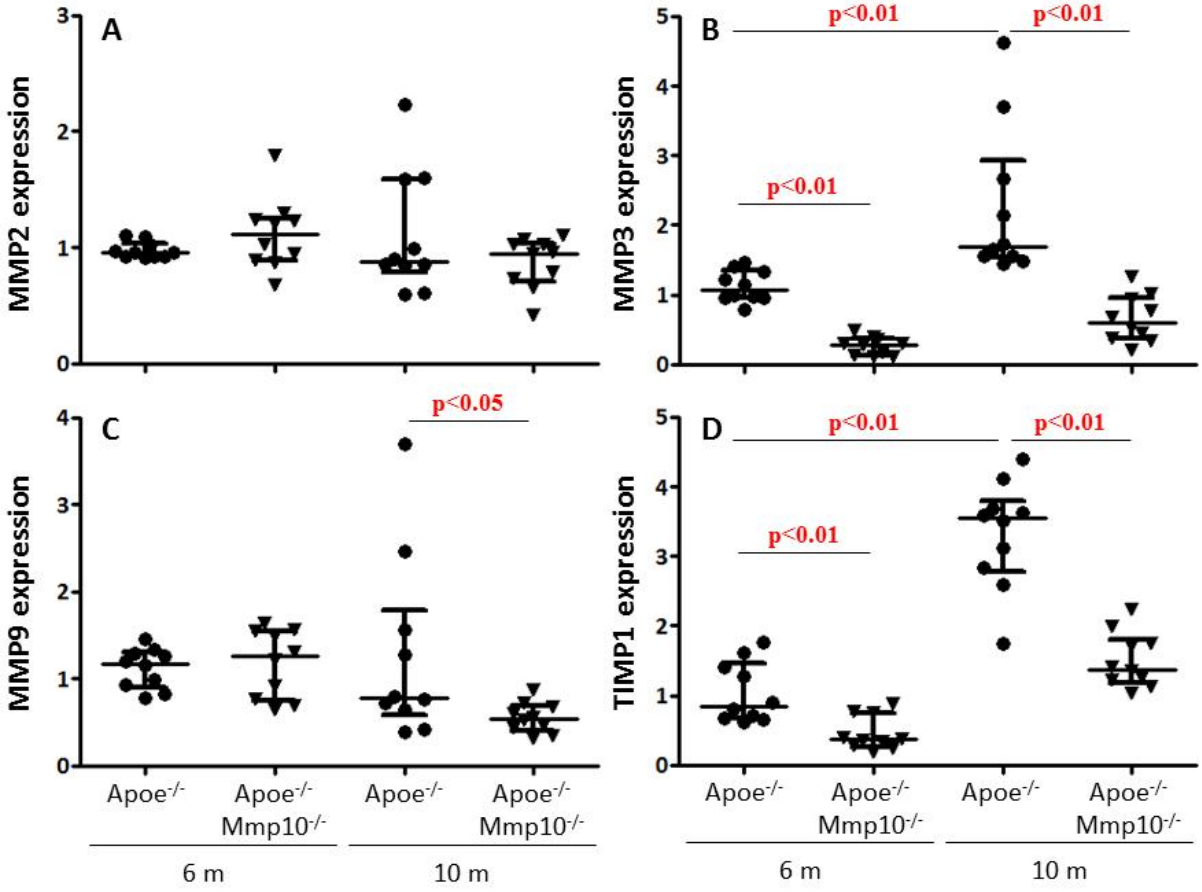

Supplemental figure 4. Altered mRNA expression of MMP2, MMP3, MMP9, and their inhibitor TIMP1 (**A**-**D**) in atherosclerotic plaques from *Apoe*$^{-/-}$*Mmp10*$^{-/-}$ mice. Median and interquartilic range; n=10.

Supplemental figure 5

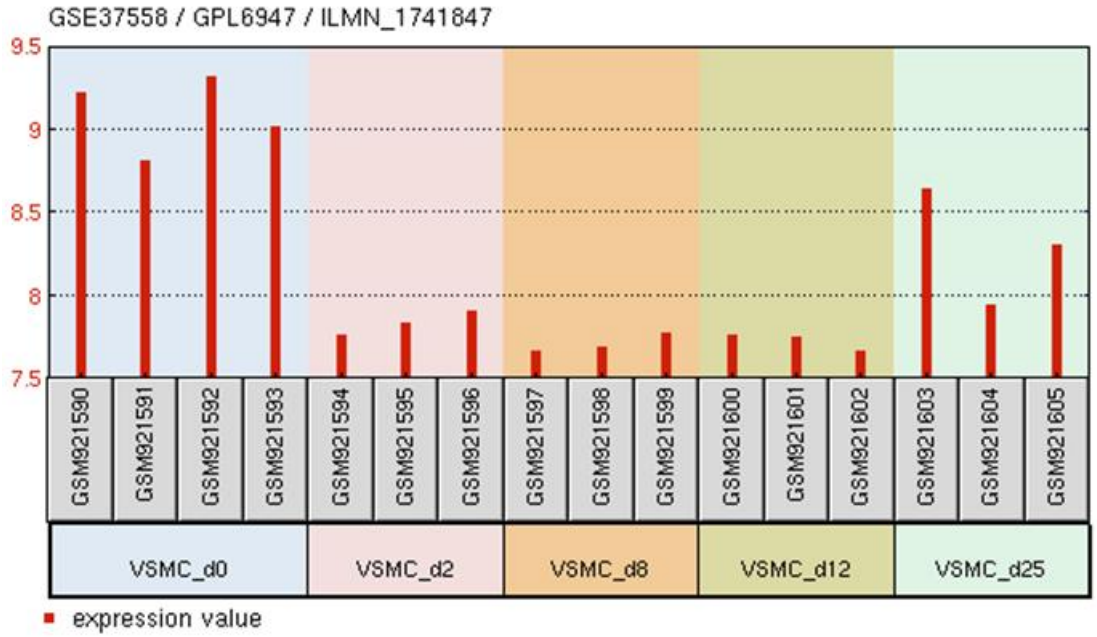

Supplemental figure 5. MMP10 expression in human coronary artery smooth muscle cells: undifferentiated (VSMC_d0) or cultured in osteogenic differentiation medium for 2 (VSMC_d2), 8 (VSMC_d2), 12 (VSMC_d2) or 25 (VSMC_d2) days. The transcriptional profile was retrieved from the Gene Expression Omnibus (GEO accession number GSE37558)[6] and analyzed with GEO2R.

References

[1] A. Leclercq, X. Houard, S. Loyau, M. Philippe, U. Sebbag, O. Meilhac, J.B. Michel, Topology of protease activities reflects atherothrombotic plaque complexity, Atherosclerosis. 191 (2007) 1–10. doi:10.1016/j.atherosclerosis.2006.04.011.

[2] H.C. Stary, A.B. Chandler, R.E. Dinsmore, V. Fuster, S. Glagov, W. Insull Jr, M.E. Rosenfeld, C.J. Schwartz, W.D. Wagner, R.W. Wissler, A definition of advanced types of atherosclerotic lesions and a histological classification of atherosclerosis. A report from the Committee on Vascular Lesions of the Council on Arteriosclerosis, American Heart Association, Arterioscler. Thromb. Vasc. Biol. 15 (1995) 1512–1531.

[3] J. Orbe, J.A. Rodriguez, R. Arias, M. Belzunce, B. Nespereira, M. Perez-Ilzarbe, C. Roncal, J.A. Paramo, Antioxidant vitamins increase the collagen content and reduce MMP-1 in a porcine model of atherosclerosis: implications for plaque stabilization, Atherosclerosis. 167 (2003) 45–53.

[4] S.Y. Kassim, S.A. Gharib, B.H. Mecham, T.P. Birkland, W.C. Parks, J.K. McGuire, Individual matrix metalloproteinases control distinct transcriptional responses in airway epithelial cells infected with Pseudomonas aeruginosa, Infect. Immun. 75 (2007) 5640–5650. doi:IAI.00799-07 [pii].

[5] R. Villa-Bellosta, J. Rivera-Torres, F.G. Osorio, R. Acin-Perez, J.A. Enriquez, C. Lopez-Otin, V. Andres, Defective extracellular pyrophosphate metabolism promotes vascular calcification in a mouse model of Hutchinson-Gilford progeria syndrome that is ameliorated on pyrophosphate treatment, Circulation. 127 (2013) 2442–2451. doi:10.1161/CIRCULATIONAHA.112.000571 [doi].

[6] R.D.A.M. Alves, M. Eijken, J. van de Peppel, J.P.T.M. van Leeuwen, Calcifying vascular smooth muscle cells and osteoblasts: independent cell types exhibiting extracellular matrix and biomineralization-related mimicries., BMC Genomics. 15 (2014) 965. doi:10.1186/1471-2164-15-965.